Conseil Scientifique de l'IN2P3 des 30-31 janvier 2014

ILC Detector Related Activities at IN2P3

V. Boudry[a], J,C. Brient[a], M. Chefdeville[b], P.Gay[c], J.Y. Hostachy[d], Y. Karyotakis[b], D. Lacour[e], I. Laktineh[f], R. Pöschl[g], M. Winter[h]

[a] LLR, Palaiseau
[b] LAPP, Annecy
[c] LPC, Clermont-Ferrand
[d] LPSC, Grenoble
[e] LPNHE, Paris
[f] IPN, Lyon
[g] LAL, Orsay
[h] IPHC, Strasbourg

12 janvier 2014

Corresponding Author : Marc Winter
e-mail : marc.winter@iphc.cnrs.fr

Résumé

This document summarises the main achievements, on-going activities and forthcoming plans of the eight groups of IN2P3 involved in detector R&D and physics studies for the International Linear Collider (ILC) project. The latter has undergone important steps recently, which are recalled in this document to set the perspective of the activities at IN2P3. Accelerator related activities, including those of beam instrumentation, are not reported in this document.

Table of contents

1 INTRODUCTION

1.1 General remarks

The International Linear Collider (ILC) is designed to deliver electron-positron collisions at a tuneable centre-of-mass energy varying from about 200 to 500 GeV, extendable to about 1 TeV. Both beams are foreseen to be polarisable at the interaction point, where they will collide with a typical luminosity in the order of 10^{34} $\mathrm{cm}^{-2}{\cdot}\mathrm{s}^{-1}$. The ILC running parameters and conditions offer a unique opportunity to complement the physics programme of the LHC, and have triggered a strong effort of investigation to build the collider in Japan. This perspective has been recognised as of prime importance for the european HEP strategy and was integrated among its main priorities for the coming decade.

The ILC project is being carried out since nearly twenty years by a worldwide community of experts, and has reached a maturity allowing to make the start of its construction a realistic technical goal. Its studies have culminated in a Technical Design Report (TDR) [1] delivered in December 2012, which provides a detailed description of all main components of the machine. The acceleration concept relies on superconducting RF (SCRF) cavities, which have been proven to be reliably fabricated in industry with the required acceleration gradient and yield [2], as illustrated by figure 1.

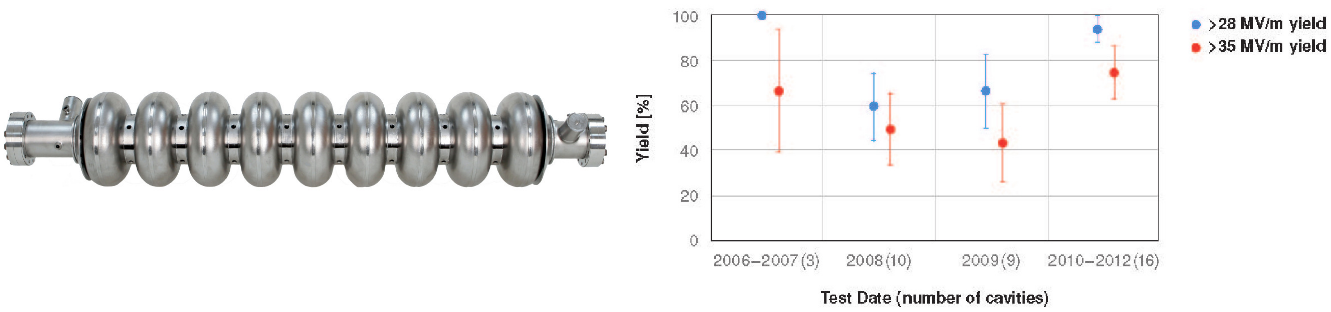

FIGURE 1 – Left : 1 m long, nine-cell 1.3 GHz superconducting niobium cavity. Right : Cavity yield for two gradient thresholds versus time for two passes using a standard prescribed treatment. The numbers in parentheses stand for the cavity sample sizes.

About 10^3 such cavities will be operated (at a gradient suited to the ILC operation up to 350 GeV at least) at the XFEL light source presently under construction at DESY and foreseen to start its physics programme in 2016 [3], providing a nearly full scale validation platform of several components of the ILC concept and implementation scheme.

The TDR also presents detailed designs of two detector concepts (ILD and SiD) developed by international teams actively pursuing the necessary R&D to validate the advanced technologies and integration concepts required to fully exploit the experimental sensitivity allowed by the collider. The complete studies underlying each concept are based on full, quite realistic, simulation and reconstruction programmes. Their results are exposed in Detailed Baseline Design (DBD) documents [4] that include the results of a variety of prominent physics studies allowing to evaluate the expected detector performances and determine the requirements of each sub-system composing the detector.

1.2 ILC running conditions

The collision energy of the ILC may be fixed at any energy between 200 GeV and its maximum energy (500 GeV in its baseline design, upgradable to about 1 TeV) and may thus be optimised for specific final state studies. While new energy settings may come out from the findings of the LHC in the next years, some settings are already well identified, such as $\sim 250\,\mathrm{GeV}$ and $500\,\mathrm{GeV}$ for Higgs boson studies and $\sim 350\,\mathrm{GeV}$ and beyond for top quark studies. Table 1 displays some prominent parameters of the machine at various collision energies. The upgrade to $1\,\mathrm{TeV}$ assumes additional linac units. The optimisation of the machine

$\mathbf{E}_{cm}$ **[GeV]**	250	350	500	1000
Peak luminosity [10^{34} cm^{-2} s^{-1}]	0.75	1.0	1.8	3.6/4.9
Fraction of luminosity in top 1%	87.1%	77.4%	58.3%	59.2/44.5%
Repetition rate [Hz]	5	5	5	4
Average accelerating gradient [MV/m]	14.7/31.5	21.4/31.5	31.5	38.2/39.2
Beam pulse duration [ms]	0.73	0.73	0.73	0.90
Number of BX per train	1312	1312	1312	2450

Table 1 – Top level operating parametres of ILC at various collision energies. The two values of acceleration gradient at energies below 500 GeV reflect the still open options for the collider staging strategy.

design, including power and cost saving, have resulted in a specific beam time structure mainly driven by the SCRF cavity properties. The machine is operated with nearly 1 ms long trains composed of about 1300, 600 ns apart, bunch crossings. This property is exploited to suppress the power consumption of the experiment by power pulsing most of its sub-systems.

The luminosities mentioned in table 1 were derived within conservative machine parameter assumptions (power and cost in particular). The potential for running the machine at a higher luminosity has been investigated, indicating that a luminosity enhancement by a factor of at least four seems achievable.

1.3 Prominent physics motivations

The ILC offers a unique opportunity to address utmost fundamental questions raised by the LHC-discovered Higgs boson as well as those related to intrinsic limits of the Standard Model (SM) or triggered by observations going beyond them, such as Dark Matter or baryon-antibaryon asymmetry.

The machine exploitation will be organised in a flexible, staged, way, where the first step is anticipated to focus on the Higgs boson, with a collision energy around 250 GeV. Very precise measurements of numerous properties of the boson will be performed, and their consistency with the SM will be examined. The study will benefit from the high sensitivity provided by the Higgs production process of Higgsstrahlung, which does not require identifying the Higgs but relies instead on the reconstruction of the associated Z boson and on the precise kinematical reconstruction of its recoil mass, based on the accurate knowledge of the collision energy.

The Higgs couplings can therefore be derived in a model-independent way [1]. Moreover, the Higgs quantum numbers (e.g. J^{PC}) will be derived without ambiguity, for instance by scanning the Higgs production threshold below $250\,\mathrm{GeV}$.

A still more comprehensive understanding of the Higgs properties will become accessible as the collision energy and luminosity progressively increase, allowing to exploit the Higgs production through WW-fusion and giving rise to an accurate measurement of the coupling to the top-quark as well as to check the existence of the Higgs self-coupling predicted by the electro-weak theory. The combination of WW-fusion and Higgsstrahlung related measurements will allow deriving the Higgs total width, predicted to be as narrow as

1. Complementary to the LHC, where Higgs boson observables are either ratios of branching ratios or measured rates, proportional to cross sections times branching ratios.

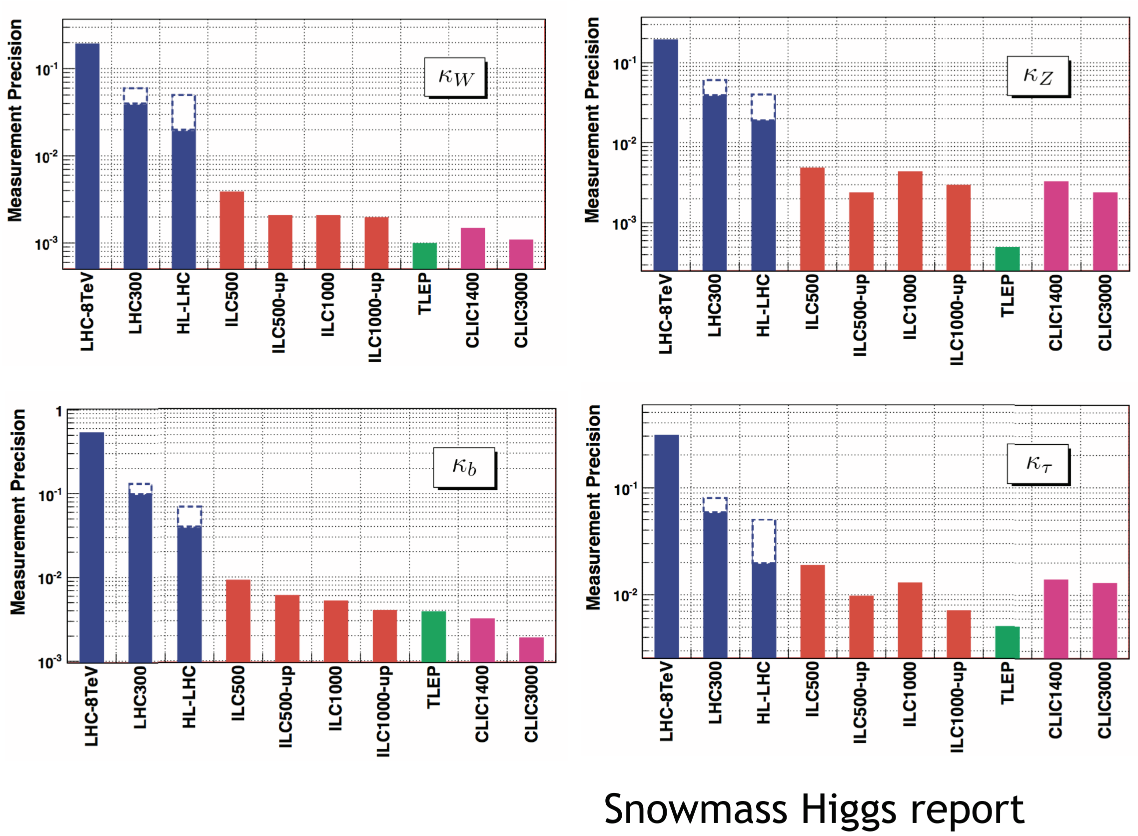

FIGURE 2 – Measurement precisions on Higgs-couplings to the W- and Z-bosons as well as to the b-quark and tau-lepton, expected from various stages of ILC and LHC, as evaluated during the Snowmass 2013 workshop, which also examined the potential of TLEP [5].

4 MeV in the SM. Ultimately, several couplings are expected to be determined with an accuracy better than 1 %, including the invisible width, which is intrinsically an open window to physics beyond the SM (BSM). Figure 2 illustrates the precision achievable on a representative set of Higgs couplings and compares it to the precision expected at the LHC. These results were obtained at the occasion of the recent Snowmass process in the US, where the ILC physics potential was examined in detail by physicists from all three regions and triggered strong interest from the US community.

All ILC measurements tend to be limited by statistics. Any improvement in the luminosity will therefore benefit directly to the measurements' accuracy (e.g. Higgs self-coupling). The physics performance of the detectors exposed in the TDR (or DBD) are nearly entirely based on a nominal luminosity not exploiting the full potential of the machine. The exploratory machine studies (mentioned earlier) leading to about 4 times more luminosity would straight away result in twice more precise physics observable measurements.

Several of the physics performance results exposed in the DBD, and earlier in the LoI [6, 7], rely on studies (often PhDs) performed by IN2P3 groups, which were particularly active in topics related to the Higgs-boson and top-quark properties assessments (see Appendix A). Some of these studies were accompanying detector developments and guided the determination of their requirements.

1.4 Overview of detector concepts

The ILC physics programme requires multi-purpose detectors with significant performance advances over past collider detectors, in particular in terms of precision. With a machine environment that is much milder than LHC standards, designs and technologies unthinkable at the LHC can be realised. In spite of this advantage, there are special issues with the ILC environment which must be addressed, the pulsed embbeded readout electronics of the detector being one of the most essential and demanding.

High-resolution jet energy and flavour reconstruction and di-jet mass determination performance are among the critical requirements. The particle flow algorithm (PFA) reconstruction technique has been developed to meet this challenge. Highly granular electromagnetic and hadron calorimeters are deployed to achieve the needed jet energy resolution of a few per-cents for 100 GeV jets, a goal set by the need to separate W and Z di-jet final states. The charged track momentum resolution requirement is set by the reconstruction of a recoiling Higgs boson associated with a Z boson decaying into a lepton pair. Challenging flavour and quark-charge tagging require a new generation of vertex detectors. The highly granular calorimeters supply particle identification and muon detection is aided by the iron return coil.

A detector R&D programme undertaken within a globally coordinated effort has been carried out since many years and has already proven the realism of several critical elements for the ILC scientific goals. Two full detector design concepts are being developed (called SiD and ILD), based on these detector performances. They are assumed to provide concurrent operation in push-pull mode sharing the sole interaction region, offering complementary approaches, cross-checks for results confirmation, reliability and insurance against mistakes. The main differences between the two detector designs originate from their overall sizes and central tracker approaches. The significantly different tracking technologies along with the compact (SiD) versus large (ILD) designs achieve the needed, valuable detector complementarity.

SiD is a compact, cost-constrained detector made possible with a 5 T magnetic field and full silicon tracking. Silicon enables time-stamping on single bunch crossings to provide robust performance, derived from immunity to spurious background bursts. The highly granular calorimeter is optimised for particle flow analysis. Flavour tagging is achieved with a very light and highly granular vertex detector relying on new pixel technologies.

ILD is a large detector with robust and stable performance over a wide range of energies. The concept uses a primary tracking system based on a continuous readout time projection chamber (TPC) to achieve excellent efficiency and robust pattern recognition performance (more than 200 hits per traversing particle).

Some silicon trackers complement the TPC coverage and reinforce track linking with surrounding sub-systems. A highly granular calorimeter system contained inside a 3.5 T magnetic field provides very good particle flow reconstruction. The vertex detector benefits from track seeding made possible in the TPC, resulting in less demanding time resolution requirements than in SiD.

Figure 3 displays the CAD picture of both detector concepts as developed for the DBD.

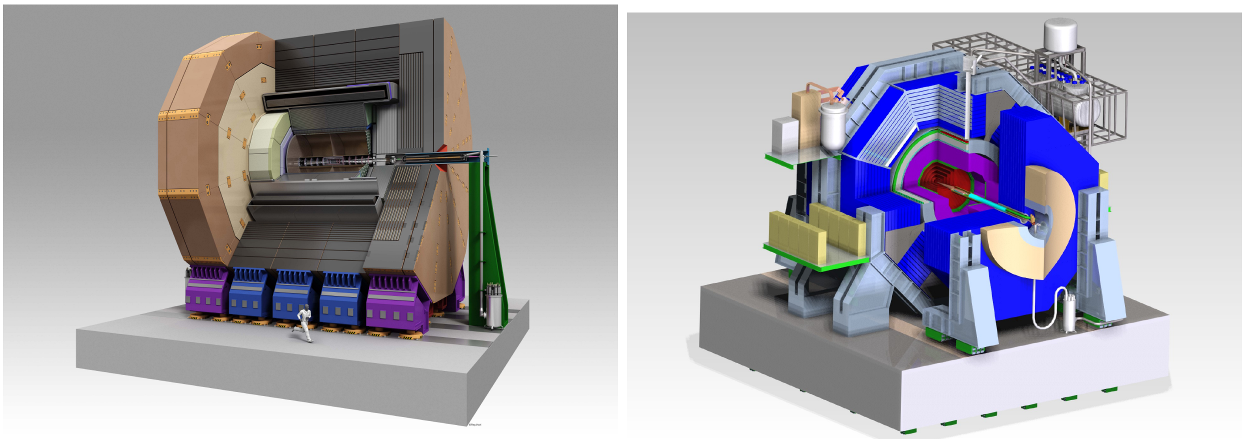

FIGURE 3 – CAD representations of the ILD (left) and SiD (right) concepts.

1.5 IN2P3 areas of activity

Eight IN2P3 laboratories (IPHC, IPNL, LAL, LAPP, LLR, LPCC, LPNHE, LPSC) are involved since at least a decade in R&D activities and physics performance studies addressing a detector suited to the ILC. They have played a prominent role in providing input and writing the Letters of Intent [6, 7] and the DBD of both detector concepts [4], with a stronger involvement in the ILD concept.

Most of the R&D effort is invested in electromagnetic and hadron calorimetry. The vertex detector and beam instrumentation are the purpose of two other R&D activities. At the occasion of the DBD, IN2P3 members have also been involved in studies addressing the detector integration and the costing, as well as in editing the document. They provided common tools and developed Particle Flow reconstruction techniques. For completeness, the IN2P3 activity on the machine is to be mentioned, which concerns mainly the key features of the SCRF cavities' powering based on specific klystrons. Several R&D studies were carried out within EU projects, such as EUDET until 2010 and, since 2011, within the AIDA project with more modest resources. Two ANR programs have supported the R&D activities addressing the hadron (DHCAL) and electro-magnetic (ECAL) calorimeters (CALIIMAX-HEP).

1.6 Evolution of the ILC project in the next 3-5 years

Several sites have been proposed for hosting the ILC by all three regions involved in the project, but Japan has been the most proactive country in promoting the project towards reality since many years. As an example, several tens of Japanese Diet members have followed since more than one year regular lectures on High Energy Physics given by Japanese scientists on a monthly basis.

Within the last 12 months, important steps have been made, starting with the official delivery of the TDR to Japan Prime Minister Abe in December 2012 and the acknowledgement of the Japanese initiative by the EU strategy group for HEP. Since then, a site has been selected (Kitakami mountains) in the North of Japan, which is already being evaluated since several years. In Summer 2013 the US HEP community examined the ILC physics potential and concluded on its unique scientific perspectives. In Autumn 2013, a Japanese scientific council composed of scientists of various research areas and of industrial and political representatives recommended the ILC project to the Japanese government, stressing its outstanding scientific value. The council also underlined that detailed construction plans were still missing to properly assess the feasibility of the project, in particular of its necessary infrastructure, as well as its adequacy with the economic policy of the country.

While the Japanese government is being creating a specific financing line for ILC in its FY2014 budget according to the request formulated by the council to realise the remaining studies, the Ministries of Research and Development (MEXT) and of Foreign Affairs (MOFA) have started a procedure of approaching representatives of each major country involved in the project, including France. The next two or three years are therefore likely to be used to take a final decision on the feasibility of the project and of its structure and share of contributions and responsibilities. In case of a positive decision, the machine construction may start around 2018, and is expected to take about nine years until completion.

Meanwhile, it is crucial that the detector R&D continues with the necessary swing to ensure resolving at least some of the remaining technical problems of the detectors, in particular as far as engineering validation and system integration are concerned. The next sections summarise the different R&D activities carried out at IN2P3, some of their major achievements and their most prominent goals in the upcoming years, together with some of the necessary means to meet them.

2 CMOS SENSOR BASED VERTEX DETECTOR

The ILC physics goals and running conditions require a vertex detector based on a pixel sensor technology and on thermo-mechanical performances differing significantly from those in use, in particular at LHC. The PICSEL group of IPHC [8] develops since many years CMOS Pixel Sensors (CPS) as well as ultra-light pixelated ladders and a specific vertex detector concept taking advantage of CPS to comply with the ILC requirements.

2.1 Physics objectives and detector requirements

The prominent reason to develop a specific pixel sensor technology and an ultra-light detector concept is the particularly high impact parameter resolution required at the ILC to comply with the ambitious flavour tagging capability. The ambitioned resolution is typically 2-3 (resp. 3-10) times better than the one achievable with an ATLAS-IBL layer in the plane transverse to (resp. containing) the beam lines. On the other hand, the required read-out speed and radiation tolerance are several orders of magnitude less demanding than at LHC.

The sensor spatial resolution should be better than 3 μm, the ladder material budget should not exceed 0.15% X_0 (or 0.3% X_0 in the double-sided geometry) and the inner detector radius should be below 2 cm. To be compatible with air flow cooling, the total power consumption should not exceed a few tens of W in average. The PICSEL group develops pixel sensors, detector ladders and a detector geometry matching these requirements.

2.2 Geometry and concept developed at IPHC

The vertex detector geometry constituting the framework of the studies is composed of three, nearly cylindrical, double-sided layers (see figure 4), equipped on both sides with 50 μm thin CPS. This geometry is the baseline of the ILD concept [4]. A major difficulty consists in reconciling the required spatial resolution and read-out speed, since the former calls for small (and therefore numerous) pixels while the second calls for the smallest possible number of pixels to read out. The concept developed at IPHC resolves the conflict by sharing the two functionalities among the two (innermost) ladder sides (see figure 4).

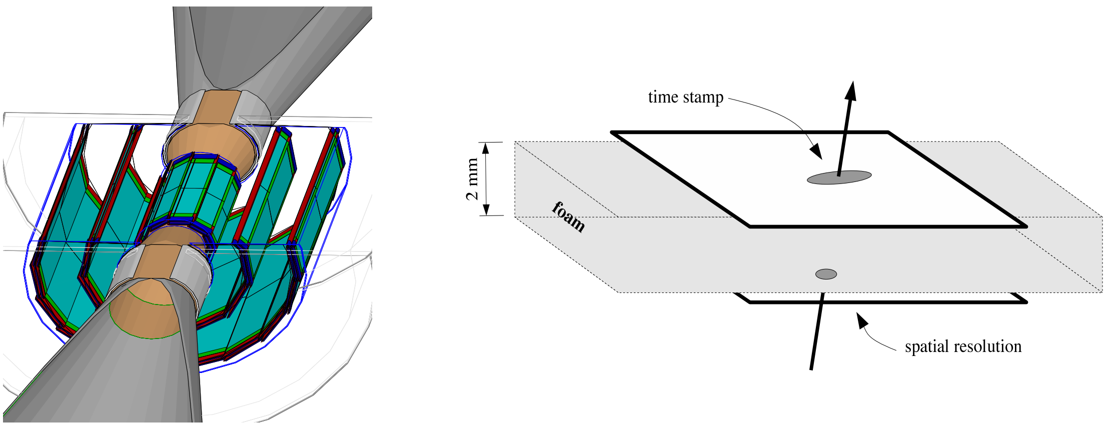

FIGURE 4 – Left : ILD vertex detector baseline geometry, relying on double-sided ladders. Right : Schematic view of the sharing concept between spatial resolution on one ladder side and timestamping on the other side.

Besides the requirements reflecting the physics goals, the detector has to face stringent requirements due to the running conditions close to the IP. The beam related background, dominated by beamstrahlung $e^{\pm}$ generated by the strong focusing and high density of the colliding bunches, induces a hit rate imposing a read-out frequency several orders of magnitude faster than required by the production rate of the signal final states alone (few Hz). The read-out time should therefore be kept in the order of a few tens of microseconds in the innermost layer, where the hit density is highest. This requirement, which tends to conflict with the demanded spatial resolution, may be alleviated for the outer layers, where a read-out time of $\sim 100\ \mu s$ is compatible with the strongly suppressed background hit rate (because of their low momentum, beamstrahlung $e^{\pm}$ are swept away by the experimental magnetic field).

Three different CPS variants are developed at IPHC. Two of them are intended to equip the two faces of the innermost layer, while the third sensor is devoted to the outer layers.

2.2.1 Pixel sensor R&D

CPS offer an attractive solution for an ILC vertex detector because of their low material budget due to their $\sim$ 20-30 μm thin (high resistivity) sensitive volume, of the possibility to implement a high density sensing node lattice (leading to high spatial resolution) and of the possibility to integrate the full signal processing circuitry on the same substrate as the sensitive volume [9]. Detailed information on the different sensor designs and test results is provided in numerous publications which may be found on the PICSEL group home page [8]. This section concentrates on those aspects which are most essential for the validation of the CPS technology and for their application to an ILC vertex detector.

The proof of principle of CPS for subatomic physics experiments was achieved with the MIMOSA-26 sensor, developed for the beam telescope of the EU project EUDET [10]. The sensor architecture is based on a column parallel read-out with amplification and correlated double sampling inside each pixel. Each column is terminated with a high precision discriminator and is read out in a rolling shutter mode in 115 μs. Despite the binary charge encoding, the spatial resolution obtained with the 18.4 μm pitch of MIMOSA-26 is close to 3 μm (see figure 5).

This architecture was extended to a sensor (MIMOSA-28) [11] adapted to the PXL vertex detector of the STAR experiment at BNL, which is being equipped with 400 sensors exhibiting a 2x2 cm^2 sensitive area, thinned to 50 μm and air cooled [12]. The m.i.p. detection efficiency observed at 30°C is displayed on figure 5 (right) as a function of the discriminator threshold and for a combined radiation load well above the ILC requirements [2]. Marginal performance variations are observed after irradiation, which validate the sensors for the radiation tolerance required at the ILC. The STAR-PXL is the pioneering detector for the CPS technology, based on ladders featuring a material budget of 0.37% X_0. An engineering prototype, composed of 3 complete sectors (out of 10) was operated successfully for the first time at RHIC within the STAR detector in May-June 2013 with pp and ArAr collisions. The complete detector will start its first physics data taking campaign in February 2014 ; It will act as a major milestone for establishing the CPS technology for the ILC.

The design of CPS adapted to the ILC is derived from the MIMOSA-26/-28 architecture, essentially in order to accommodate the read-out time and spatial resolution. Different CPS variants are foreseen in order to reach optimal performances in each layer.

For the inner layer, the sensors are optimised for single point resolution and read-out time, relaxing the power consumption constraint. The conflict between high granularity and fast read-out is resolved by equipping each ladder with two different types of sensors, one achieving the required spatial resolution and

2. $\lesssim$ 100 kRad and 10^{11} n_{eq}/cm^2 at 500 GeV.

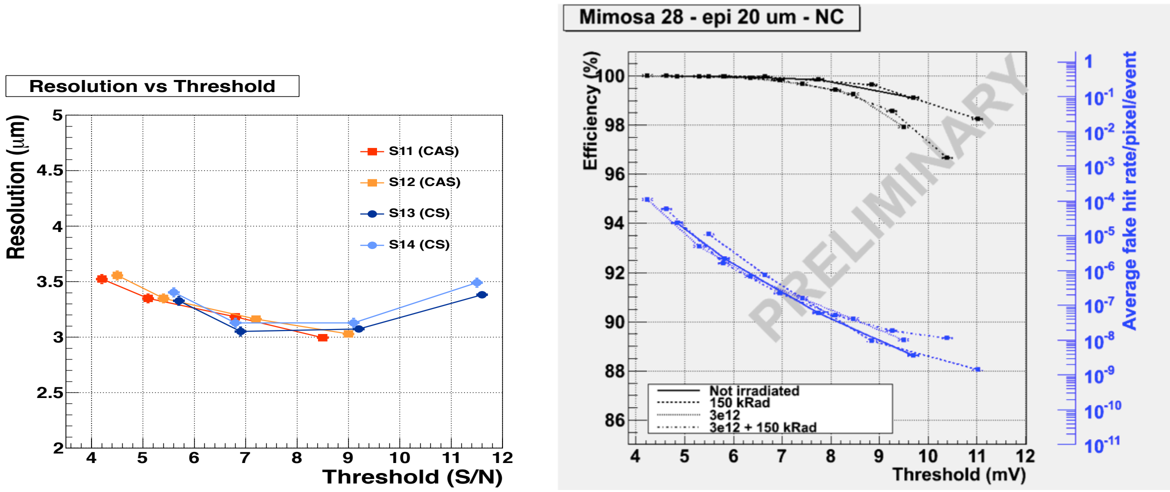

FIGURE 5 – Left : measured single point resolution for a 18.4 μm pitch as a function of the discriminator threshold (the colours refer to in-pixel circuitry variants). Right : measured variation of the m.i.p. detection efficiency and fake hit rate (fraction of pixel noise fluctuations above threshold) of MIMOSA-28 as a function of the discriminator threshold, before an after irradiation (150 kRad, $3{\cdot}10^{12} n_{eq}/cm^2$), at a coolant temperature of 30°C.

one providing a fast time stamp. Both sensors are based on a 1-bit charge encoding achieved with on-chip high precision discriminators.

The highly granular sensors are mounted on one side of the ladders, and feature square pixels with ~ 17 μm pitch providing a spatial resolution < 3 μm. Their frame read-out time is 50 μs. The fast sensors equip the other side of the ladder. They feature rectangular pixels (e.g. $17{\times}85$ μm^2), which result in 5 times less pixels per column, and therefore in a 10 μs read-out time. The spatial resolution is $\lesssim 6$ μm because of the pixel dimensions. Medium scale prototypes (MIMOSA-30a and -30b) were fabricated and tested in 2010/2011 in ordre to validate this approach.

It follows that correlating the ~ 2 mm apart impacts of traversing particles, the latter get assigned a spatial resolution of < 3 μm and a time stamp of $\lesssim 10$ μs, which is expected to strongly suppress the perturbation of the track reconstruction due to beam related background, even in case of rates well in excess of the simulated values.

For the outer layers, the sensor design privileges power saving since these layers represent about 90% of the detector surface. This goal is achieved by enlarging the pixels in order to reduce the number of columns. The consecutive degradation of the spatial resolution is mitigated by ending each column with a 4-bit ADC. The $34{\times}34$ μm^2 large pixels foreseen deliver therefore a spatial resolution of ~ 4 μm, combined with a read-out time of ~ 100 μs. A small prototype of the sensor (MIMOSA-31) has been fabricated and tested in 2010/2012, demonstrating the validity of the approach at nominal frequency.

Overall, the detector would dissipate about 10 W in average, assuming power cycling with a 2 % duty cycle (i.e. 5 ms long periods of power dissipation centred on a 1 ms long train), a performance well compatible with air flow cooling.

The achievements above were obtained with a CMOS manufacturing technology based on a 0.35 μm feature size which did not allow exploiting the real potential of CPS. In 2011 the PICSEL group moved to a 0.18 μm CMOS technology offering more attractive fabrication parameters, motivated by the perspective of using CPS for the Inner Tracker System (ITS) upgrade of the ALICE experiment at the CERN-LHC. The prototyping performed in 2012 and 2013 has allowed reproducing all components of the MIMOSA-26 architecture in this technology to validate its modification for a twice faster read-out [13, 14].

2.2.2 Ladder developments

Double-sided ladders are being developed within a collaboration with Bristol University and DESY, based on a prototype called PLUME [3]. The main feature of the PLUME ladder concept is a double-sided layout, which consists of two sensor layers separated by a support structure [15]. A traversing particle produces two hits in the two ladder sensors. The hits, separated by approximately 2 mm, can be correlated and used to reconstruct a mini-vector with potential benefits of a better resolution, easier alignment and improved reconstruction of shallow angle tracks. The ladder concept is based on 2 sets of 6 MIMOSA-26 sensors (8 million pixels in total) thinned to 50 μm.

A first prototype was fabricated in 2011, composed of 2 sets of 6 MIMOSA-26 chips thinned to 50 μm and mounted on thin flex cables assembled on both sides of a support structure made of SiC foam. It was successfully operated at nominal frequency. Its material budget, amounting to 0.61 % X_0, was not optimised. A new prototype is being fabricated, which features 0.35 % X_0, and is planned to be tested on beam in 2014.

2.3 Plans for the coming years

2.3.1 CPS development in 0.18 μm technology

The outcome of the R&D on CPS performed up to now is a proof of principle for all 3 sensor variants envisaged for the different layers of an ILC vertex detector. The performances obtained are satisfactory and comply with the detector requirements up to 500 GeV, but can barely accommodate standalone tracking (nor running at 1 TeV). The 0.18 μm technology used by the group for the ALICE-ITS [13, 14] allows for significantly faster read-out while simultaneously reducing the power consumption.

The main goal in the coming years is therefore to translate the 3 sensor variants described above from the 0.35 μm CMOS process used for STAR to the 0.18 μm process used for ALICE and to optimise their designs. A prominent objective is to achieve a time stamping resolution of $\lesssim 1$ μs, possibly 0.5 μs to tag individual bunch crossings in the innermost layer. This will be complemented with the development of faster outer layer sensors, based on in-pixel ADCs. Both chips designs will be derived from the ASTRAL sensors developed for the ALICE-ITS.

An alternative detector read-out approach is also being considered, based on *fine pixels* (~ 5 μm pitch) integrating signals over a complete bunch train and read out during the 200 ms separating consecutive trains. A prototype was already fabricated and will be tested in 2014. The plan would be to next realise a low power 8-bit ADC complying simultaneously with a $<$ 200 ms read-out time and an overall detector power consumption of a few tens of watts only.

2.3.2 Double-sided ladder developments and integration issues

There is still room to reduce the material budget of the PLUME double-sided ladder. Different approaches will be investigated, aiming at a target value $< 0.3\%$ X_0, possibly exploiting new materials for the support structure. A ladder associating 2 different types of sensors may also be developed, equipped with MIMOSA-26 chips on one side and with faster ($\lesssim 20$ μs) ASTRAL sensors (prototyped for the ALICE-ITS) on the other side, to test the concept of associating hits created by a traversing particle on both sides of a ladder equipped with complementary sensors..

Besides the ladder development itself, the ladders produced in 2014 will be used to address system issues. Micrometric alignment technics will be studied using sets of PLUME ladders assembled on 3 stations representing an azimuthal section of a vertex detector and installed on a beam line, possibly integrated in a work package of the successor of the AIDA project. Another important study concerns thermo-mechanical

3. standing for Pixellated Ladder with Ultra-light Material Embedding.

issues related to power cycling in a high magnetic field. Several other system integration aspects may also be studied, based on the forefront achievements coming out from the ALICE-ITS upgrade.

2.4 Resources associated to the activity

2.4.1 Personnel

The PICSEL group is composed of $\sim$ 20 staff personnel and 10 non-permanent members. The former are predominantly chip designers (11 engineers) and electronics engineers (5 engineers). The 4 physicists of the group are half from CNRS and half from Strasbourg University. The non-permanent members are predominantly PhD students (typically 4-6 chip designers and 1-2 physicists). There has been 1-2 post-docs in the group through the years concerned. Besides the PICSEL group, the micro-technics service of IPHC is involved in the PICSEL group projects at the level of 2 FTE in average. All together, the involvement of the personnel mentioned above adds up to typically 12 FTE·year staff involved in ILC activities and 5 FTE·year non-permanent staff.

Until 2016, the main activity of the group will address the ALICE-ITS upgrade, with a strong overlap with the ILC related CPS development. During 2016, activities directly addressing ILC may become the group main line, depending on the project evolution, and could result in a $\gtrsim$ 20 FTE·year involvement of IPHC.

2.4.2 Budget

The budget invested in ILC activities since 2008 is summarised in Appendix B, including resources allocated by IN2P3 and those obtained elsewhere (essentially CPER and EU).

The budget required to pursue the R&D for the ILC until 2016 will concentrate on integration aspects since the sensor R&D is essentially driven by the ALICE-ITS upgrade. Some dedicated ILC chip prototypes may however be fabricated (e.g. in-pixel ADC, elongated pixels for 1 μs time stamping), demanding an annual contribution of $\sim$ 15-20 keuros. The system developments (mainly ladder production) require 10-15 keuros per annum. Test PCBs and equipment need yearly 10-15 keuros including test benches maintenance. Finally beam tests and meetings require a budget of 30-40 keuros per year. Overall, the annual budget required is about 70-80 keuros, out of which 20-30 keuros are likely to be found among collaborators. **The yearly budget required from IN2P3 for ILC activities on the vertex detector in the coming 2-3 years is therefore about 50 keuros**.

3 SILICON TUNGSTEN ELECTROMAGNETIC CALORIMETER

For use as a particle flow detector, the ECAL must have excellent two-particle separation (down to distances of a few cm) and a reasonably good single photon energy resolution, not worse than around $20\,\%/\sqrt{E[\mathrm{GeV}]}$. Two-particle separation is achieved by a highly segmented readout together with a minimisation of size of electromagnetic (EM) showers. A sampling calorimeter with tungsten absorber and thin, highly segmented sampling layers can provide such performance. The small Molière radius and radiation length of tungsten give compact EM showers, while its relatively long hadronic interaction length also gives some natural separation between EM and hadronic showers. The sampling layers must have a small thickness (to reduce the overall Molière radius) and be easily segmented (at the level of 5 mm) in order to give the necessary readout granularity. These requirements can be satisfied by silicon sensors. Matrices of PIN diodes made in $\sim 300-500\,\mu$m-thick high resistivity silicon, typically $5\,\mathrm{k}\Omega \cdot \mathrm{cm}$, can be fully depleted by the application of a modest reverse bias voltage (100-200 V).

The results and realisations presented in the following have been nearly exclusively achieved by the involved IN2P3 groups, LLR, LAL, LPSC, LPNHE, LPCC and the OMEGA microelectronics group. The work is well integrated into the international R&D collaboration CALICE. In particular a close collaboration with Japanese groups is now established. The R&D work was supported by the European Framework programs EUDET and AIDA as well as by the French ANR (CALIIMAX-HEP). In case of a positive development towards the ILC, the R&D work will be progressively integrated into the emerging detector collaborations ILD and/or SiD.

In the following only a list of publications is given. Where possible overview articles have been chosen. Further information can be found under http://flc.web.lal.in2p3.fr/poeschl/cs-in2p3-ecal-pub.pdf.

3.1 Detector prototypes

The so-called *physics prototype* [16], shown in Fig. 6 has been operated between 2004 and 2011 and aimed at demonstrating the ability of such an ECAL to meet the performance requirements. It has an active area of $18 \times 18\,\mathrm{cm}^2$ and 30 sampling layers. The active sensors has a granularity of $1 \times 1\,\mathrm{cm}^2$, giving a total of nearly 10 k readout channels.

A second, *technological prototype* is presently under development [17] : it features a ILD-barrel type Tungsten-Carbon Fibre structure holding 14 shorts sensor units (or SLABs) to form a detection tower, and a long SLAB (see Fig. 8 left). The auto-triggered, power-pulsed, readout electronics is embedded in the SLABs. This prototype is used to develop and test the technologies required to integrate an ECAL into a larger detector, and to prepare for the eventual construction of a full detector, including some key aspects of industrialisation.

3.2 Elements of the R&D and main conclusions

3.2.1 Physics prototype

The stability of the physics prototype is well demonstrated by the results of the periodic calibrations of all detector channels. The calibration factors found were stable over long time periods to the % level, and showed no influence from external factors [16]. Calibration studies were performed in three PhD theses since 2008.

No major systematic problems were identified with the concept of this detector or with its technical design. The signal-over-noise ratio in the physics prototype was measured to be 7.5 :1 [16], which is already sufficiently close to the final R&D goal of 10 :1. The value 7.5 :1 was confirmed over the years and even increased to 10 :1 for some elements of the technological prototype. Note at this point that the primary goal

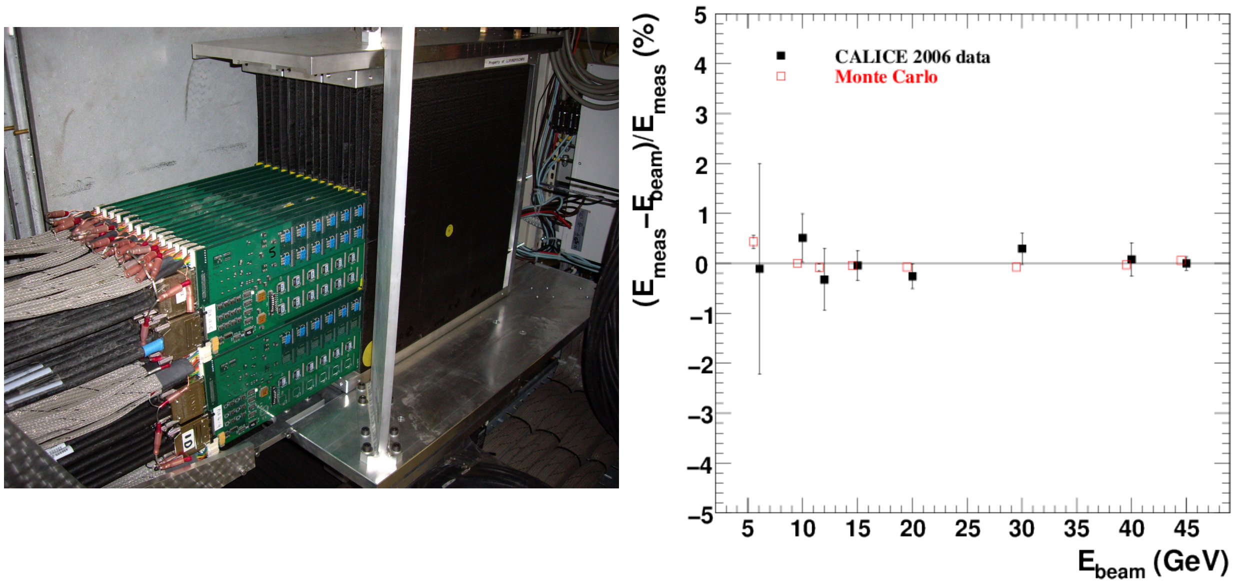

FIGURE 6 – Left : the SiECAL physics prototype. Right : linearity of the energy response, as measured in both real data and simulation.

of the calorimeter is not an excellent energy resolution but to assure a high granularity for the application as a Particle Flow calorimeter.

An overview on beam test results is given in [18]. Details can be found in the list of citations given above. The response of the physics prototype to electrons is found to be linear to within 1% in the energy range between 1 and 45 GeV, as shown in Figure 6. The energy resolution for electrons was measured to be $16.6/\sqrt{E(\mathrm{GeV})} \oplus 1.1\%$. Both the energy response and the longitudinal shower profiles of electron showers are well described in the simulation, as is the effective Molière radius.

The data collected with hadron beams have been used to constrain the models for hadronic showers implemented in GEANT4 version 9.3, with the FTFB_BERT physics list giving the best description of the data. The for pions in an energy range between 8 and 80 GeV has been extended within a PhD thesis to the range 2 to 10 GeV and will be published soon in a journal paper. Analysis of overlaid "MIP"-like and EM shower events shows that the efficiency to distinguish them (in the ECAL alone) begins to decrease at a separation of 3 cm, to a minimum of around 50% for overlapping particles.

3.2.2 Technological prototype

Figure 7 shows a schematic view of the technological prototype : The mechanical housing is realised by a tungsten-carbon reinforced epoxy (CRP) composite, which supports at the same time the absorption medium and ensures the mechanical integrity of the detector.

Mechanical structures After a 5-year program and following a semi-industrial procedure, a large prototype structure has been produced in 2012, close in scale to a barrel module for ILD (see Fig. 8 middle). It features 15 × 3 1.5 m-long alveola interleaved with Tungsten plates. A deviation from planarity on the top side of the structure of only about 5 mm was measured. Though tolerable for a module for a full detector, the assembly procedure will be revised in order to achieve an even better planarity of the structure.

FIGURE 7 – Left : Schematic view of the technological prototype with dimension. Center : Mechanical structure of the technical prototype with a short slab in front and one inserted on the right. Right : 2.5 m alveolar end-cap layer.

For the end-caps longer structures are required and the orientation of modules is different to those in the barrel. The weight of the tungsten exerts a shear force on the horizontal alveolar structures and studies are continuing to assure the required strength of the thin alveolar walls.

As shown on the right part of Fig. 7, some long alveolar layer prototypes have been moulded in order to validate the technological specific production process and to allow the design of adapted tools for long draping in the context of industrialisation. In parallel, an integrating tool for barrel and end-cap modules (up to 2.5 t) via their fine supporting rail system is under construction.

In the future the industrialisation aspect of production process (~ 675 cells up to 2.50 m), the optimisation of finite element simulations on global mechanical behaviour shall be finalised. Concerning the composite structure several topics are still to be addressed in order to validate the moulding process of large structures. Due to the multiple shapes of end-cap modules, one assembling mould should be designed soon. A program of tests (shearing, delamination, bending of modules according rails specification, etc.) will validate global and local simulations.

The left part of Fig. 8 shows a cross section through two calorimeter layers which form a slab. The sensitive parts will be mounted on both sides of tungsten board embedded in an "H" made of carbon fibre, equipped with a thermal drain, wrapped and inserted into the alveoli of the mechanical structure. The front end electronics is integrated into the detector layer. Beam test measurements with high energy electron showers have shown that this does not compromise the quality of the delivered signals [19].

The silicon sensors are the central component of the detector, and also the most expensive. Work is ongoing on the sensor design, particularly on the sensor edge. Silicon sensors of various designs and producers have been purchased. These include large $9 \times 9\,\mathrm{cm}^2$ sensors from Hamamatsu Photonics as shown in the right part of Fig. 8. The Hamamatsu sensors have excellent electrical characteristics, and a number of them have been successfully tested in beam tests. An undesirable feature was identified in beam tests with the physics prototype : a large energy deposition near the guard rings provokes a cross-talk between the (electrically floating) sensor guard rings and the pixels at the sensor edge. Dedicated numerical and experimental studies on "baby wafers" of the effect have shown that the effect can at least be attenuated by about a factor of 80 by segmenting the guard ring [20].

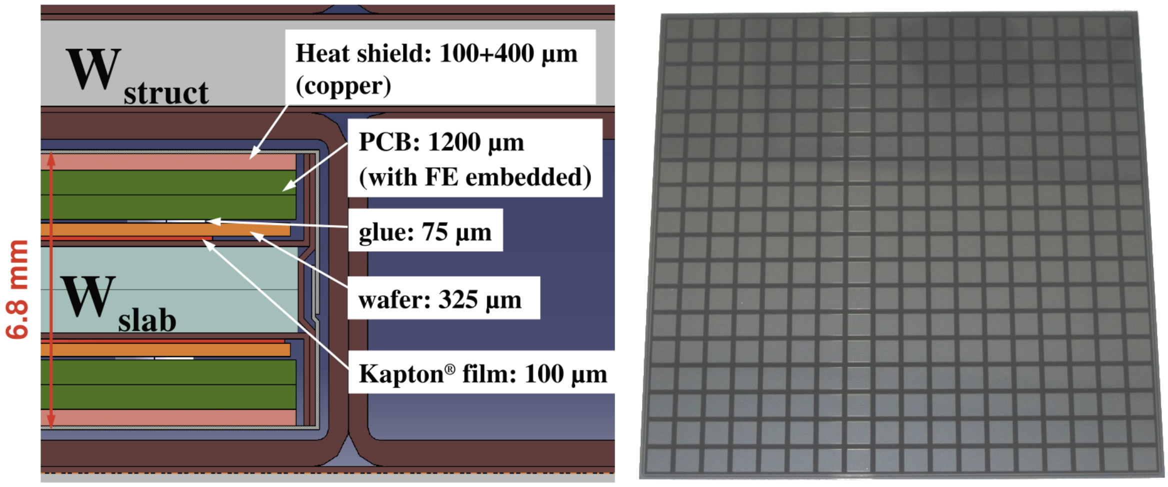

FIGURE 8 – Left : Cross section through one slab of the prototype with the thickness of the various components. Right : Hamamatsu Photonics silicon sensor : 324 pixels of $5 \times 5\,\mathrm{mm}^2$.

Recent tests with an infrared laser shooting in the guard-ring reproduced the cross-talk effect, opening the way to a validation of the design on a test bench. A precise scan of the edge of the wafer is foreseen in 2014 at the PHIL accelerator in Orsay, on a dedicated SLAB.

Simpler and/or "open" designs, which could then be manufactured by non-specialist companies and therefore reducing the sensor cost, have been developed. Direct discussion with Hamamatsu Japan through the U. of Tokyo and U. of Kyushu, allowed for relaxing some of the requirements on the wafers. An offer close to the price tag aimed at in the DBD ($2.5\,\mathrm{EUR/cm}^2$) was done this year. This was done in the framework of a MoU between CNRS and U. of Kyushu.

Readout electronics The silicon pads are read out by the SKIROC2 ASICS, designed by the OMEGA group in AMS SiGe $0.35\,\mu\mathrm{m}$ technology and integrating 64 identical channels [21]. Each channel has been designed to handle a large dynamic range, from 1/2 MIP (about 2 fC for a $325\,\mu\mathrm{m}$ thick wafer) up to 2500 MIPs (10 pC). The chip allows auto triggering on 1/2 MIP and integrates the analogue storage and the digitisation. Each of the 64 channels has an input charge preamplifier. A common gain for all channels can be set by slow control. Each preamplifier is followed by a slow channel for the charge measurement and by a fast channel for trigger generation. The charges are stored in switched capacitor arrays, converted by a 12-bit Wilkinson ADC and sent to an integrated 4 Kbytes memory. Each stage of the ASIC can be periodically shut down, meeting therefore the design requirement of the ILC that the front end electronics should be power pulsed in order to control the power budget of an ILC detector. A power consumption of $27\,\mu\mathrm{W}$/channel is reported for the power pulsed mode

An alternative to SKIROC2 may be the CaloRIC ASIC [22]. CaloRIC is based on a fully differential and synchronous architecture, designed with a pure CMOS technology. Similar to SKIROC2 it performs the complete processing of the signal delivered by the Si-PIN diode of the detector. CaloRIC comprises a variant-filter based on a gated-integrator and a 12-bit ADC, based on a cyclic architecture. Measurements of the first prototype of CaloRIC show a global integral non-linearity better than 0.2% for low energy particles, and limited to 2% for high energy particles. The measured Equivalent Noise Charge (ENC) is evaluated at 0.6 fC, which corresponds to 1/6 times the signal released by a Minimum Ionising Particle (MIP). With the timing sequence of the ILC, the power consumption of the complete channel is evaluated at $43\,\mu\mathrm{W}$ using power pulsing.

Note also that a pipeline ADC has been developed in [23]. A 14 bit up to 15 MSPs DAC in CMOS 0.35µm process technology has been designed and tested for the calibration chain [24]. This prototype is designed for integration into the future SKIROC ASIC.

PCB Development of the PCB that carries the silicon sensors and SKIROC2 ASIC has been somewhat problematic, due to the stringent requirements on the board thickness ($\lesssim 1.2$ mm), together with its rather large area. This has given rise to problems with the planarity of prototypes received so far. Thin PCBs with wire bonded unpackaged ASICs incorporated into the PCB volume have already been produced and are operational but they don't meet the specifications on planarity.

To limit the risks and complete the prototype, an alternative PCB using BGA packaged chips and with relaxed constraints on the thickness (1.7 mm) was recently produced and is currently tested. It respects the planarity at the cost of the additional thickness of packaging (to be reduced in future version), and a reduced number of sensor layers in the technological prototype but allows shorted signal paths and chip testing.

SLABs A calorimeter SLAB of up to 2.5 m in length will be composed of upto ten so called Active Signal Units or ASUs, where an ASU is the entity of silicon wafer, PCB and readout ASIC. A technique to interconnect the ASUs has been developed and applied successfully. The fragile ensemble has to be inserted into the alveolar structure which houses the calorimeter layers. The integration cradles are under development and a first integration test with a demonstrator has been successfully conducted.

The SLAB assembly includes the gluing of the wafer to the PCB using a robotic system. The gluing is a delicate procedure and its success puts tight requirements on the shape in particular of the PCB. A complete chain of quality control for each item entering the fabrication of the SLABs is being set-up.

Cooling A cooling system has been developed and is available for the large scale prototype [17]. A heat exchanger will be coupled to a copper drain at the outer part of the Ecal layers. The copper drain ensures the heat evacuation of residual heat from the inner parts of the detector layers. Due to a small temperature gradient of maximal 6° C along an Ecal layer, the concept of applying cooling only at the detector extremity seems to be appropriate. Out of the local cooling system, the global thermalisation system with its cooling station is also in progress. Several leak-less loops at real scale (9 m, 11 m and 13 m high) are under construction. The design of the control system is under study.

The real scale prototype of the leak-less loop will have to validate the cooling solution adopted for the whole ECAL ; a further step including the connection to the full local circuit with heat exchangers on a module will allow for finalising thermal tests representative of power variations (limits of pulsing).

Beam test Beam tests with up to eight short SLABs have been performed in 2012 and 2013, see Fig. 9. These SLABs were equipped with only one ASU each. A scalable and compact DAQ system [25] based on adapted ethernet protocol and HDMI cables has been brought into operation for the beam tests. The detector is configured using XML and python scripts.

In [26] the Signal-over-Noise ratio is found to be always above 10 :1 for different settings of the SKIROC2 ASIC. For a better detector understanding a simulation chain has been developed that e.g. is able to reproduce the the position of the MIP.

During the beam tests the detector was operated in *power pulsed* mode. The analysis is still ongoing but a few preliminary results are given here. Power pulsing implies a periodical shut-down and relaunch of the bias currents that polarise the various stages of the ASIC. After the relaunch a certain delay has to be taken into account until the ASIC is fully operational. Ongoing studies show that the pedestals stabilises after about

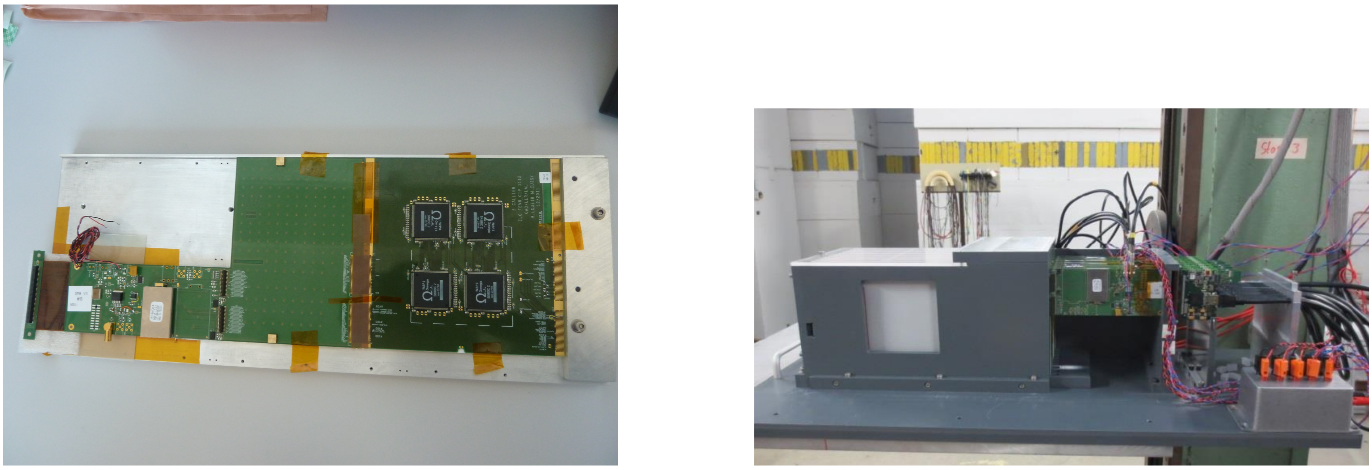

FIGURE 9 – Left : Picture of one layer of the SiW Ecal setup tested in 2012 and 2013. Right : Experimental setup at DESY.

600 μs. In future versions the delay until first signal acceptance will be set to 1 ms. The effect on the power management of the detector will have to be studied.

Further analysis reveals a good correlation between pedestals and MIP signals for a detector operation in power pulsed and continuous mode. This however requires an excellent control of all components of an ASU as e.g. assuring short connection lines between Si pads and ASICs. Note, finally that the pedestal stability in power pulsed mode has been tested in a magnetic field of up to 2 T and no variation of the pedestal and the detector noise has been observed.

3.3 Studies for the ILD

For the DBD the inner radius of the ECAL was fixed at $R_{\mathrm{TPC}} = 1.84\,\mathrm{m}$ for a "Half-Z" of 2,35 m, a thickness of $\sim 20\,\mathrm{cm}$ and 30 layers. This results in an ECAL including 140 t of W, $\sim 2600\,\mathrm{m}^2$ Si, and with $5 \times 5\,\mathrm{mm}^2$ pixels, 100 Mchannels.

In view of the driving cost of the ECAL in ILD ($\sim 30\,\%$), and the realisation that the PFA software was not tuned on a combination of a fine granularity ECAL and gaseous HCAL, a re-optimisation of the parameters was started on the two main drivers : R_{TPC} (for a fixed ratio Length/Radius) and the numbers of layers. The results shown in [27] and [28] hints that a model with a $R_{\mathrm{TPC}} \sim 1.4\,\mathrm{m}$ and 25 layers could cut the price by nearly a half for a very moderate decrease of performances of jets reconstruction (+10 % on JER).

Moreover the complete potential of the high granularity is not yet fully exploited and should bring further improvement. Several developments in PFA techniques at IN2P3 have been on-going during the last years in several labs consisting in a high performance photon reconstruction [29], identifying the tracks in the calorimeters (ECAL or HCAL) using the Hough transform [18, 30] or bushing trees [31], the fractal nature of showers [32] or extracting information using machine algorithms. Theses efforts should be brought together (an ANR proposal has been submitted for this) in order to get the best results from our detectors.

The interplay between reconstruction and detector techniques is very high in imaging calorimetry : sufficient room for software techniques improvement of the detectors performances must be left for future generations.

3.4 R&D plans and steps towards a real detector

The next few years will be used to progressively complete the technological prototype with up to 30 short ASUs and at least one long layer with up to 10 ASUs. This prototype is to be tested in beam test campaigns in the years 2015-2016.

The very next step is to produce ASUs for four wafers and read out by 16 ASICs. The final layout of the calorimeter for a linear collider detector depends significantly on the success of the PCB manufacturing. As for the sensors a close collaboration with industrial partners is needed.

The final SKIROC ASIC will feature an on-chip zero suppression. Its development will follow a staged approach, with first tests on the HARDROC3, and a SKIROC on SoI. Therefore it has been agreed to produce first an intermediate version, dubbed SKIROC2b, to assure that (minor) flaws observed with the current SKIROC2 ASIC can be completely remedied. A production run of SKIROC2b ASICs is planned for the end of 2014.

The silicon sensors are a major cost factor for the ECAL. From HPK, see also above, there exists a first (unofficial) cost estimate for a large-scale production. A larger number of silicon detector manufacturers will be needed when a full ECAL is built. Therefore, the IN2P3 is about to establish a NDA with the manufacturer LFoundry who provided a written cost estimate. Further development of links with silicon sensor manufacturers is essential in order to better understand the eventual cost of such a detector, and to prepare for possible mass production.

The use of power pulsing in the front end electronics is a central tenet of the detector design. The results obtained in the 2013 beam test campaign are very promising in this respect but need to be confirmed as the system evolves. The validation need to incorporate an estimation of the final power dissipation of the detector.

Many steps of detector construction will be outsourced to industry, and one aim of the technological prototype is to choose techniques which are well adapted to an industrial process. This however requires still scrutinising the available assembly tools and techniques as e.g. the robotic gluing system. In parallel with this, a significant quality control control process will have to be developed, with tests of detector components being carried out at various stages of their integration into detector elements.

3.4.1 Support needs in the next 2-3 years

A good fraction of major investments indicated above can be covered by existing third party funding through e.g. AIDA. Further requests for third party funding will be made within the European HORIZON2020 call and, where possible, to the French ANR. Naturally, our international partners will have their share on the needed investments. Nevertheless, the successful continuation of the activities in the next 2-3 years (and the assurance of the leadership of the French groups) will require an annual budget through IN2P3 that remains at least at the level of the requests formulated for 2014. *A major concern is the lack of staff, particularly of scientists, working on the project.*

4 GRPC AND MICROMEGAS BASED HADRON CALORIMETERS

Hadronic calorimeter (HCAL) plays an essential role in PFA-based experiments as those proposed for the ILC. It allows to separate the deposits of charged and neutral hadrons and to precisely measure the energy of the neutrals. The contribution of the neutrals to the jet energy, around 10% on average, fluctuates in a wide range from event to event, and the accuracy of the measurement is the dominant contribution to the particle flow resolution for jet energies up to about 100 GeV. For higher energies, the performance is dominated by confusion, and both topological pattern recognition and energy information are important for correct track cluster assignment. High-granularity hadronic calorimeter is thus needed to achieve excellent jet energy resolution.

HCAL proposed for both projects of ILC (ILD and SiD), are sampling calorimeters with steel as absorber and scintillator tiles or gaseous devices with embedded electronics for the active part. The steel was chosen due to its rigidity which allows to build self-supporting structure without auxiliary supports (dead regions). Moreover, the moderate ratio of hadronic interaction length ($\lambda_I = 17$ cm) to electromagnetic radiation length ($X_0 = 1.8$ cm) of iron, allows a fine longitudinal sampling in terms of $X_0$with a reasonable number of layers in λ_I, thus keeping the detector volume and readout channel count acceptable.

The French groups involved in the two ILC projects propose gaseous detectors for the HCAL active layers : Glass Resistive Plate Chamber (GRPC) for the HCAL of ILD and MICRO MEsh GASeous detector (Micromegas). This is motivated by the excellent efficiency and homogeneity the gaseous detectors could provide. Another important advantage of gaseous detectors is the possibility to have very fine lateral segmentation. Indeed, in contrast to scintillator tiles, the lateral segmentation of gaseous devices is determined by the electronics readout.

To obtain excellent resolution of hadronic shower energy measurement using a binary readout, a lateral segmentation of few millimeters is needed. This however leads to a huge number of electronics hardly affordable for the future ILC hadronic calorimeters. 1x1 cm^2 cells were found to be a good compromise that still provides very good resolution at moderate energies. However, simulation studies show that saturation effects are expected to show up at higher energies ($> 50\,\mathrm{GeV}$). This happens when many particles cross one cell in the center of the hadronic shower. To reduce these effects, the choice of multi-threshold electronics (Semi-Digital) readout was envisaged to improve on the energy resolution by exploiting the particle density in more appropriate way.

High-granularity calorimeters imply however a huge number of electronics channels to operate them. This has two important consequences. The first is the power consumption and the resulting increase of temperature which affects the behavior of the active layers. The other consequence is the number of service cables needed to power, read out these channels. These two aspects can deteriorate the performance of the HCAL and destroy the principle of PFA if they are not addressed properly.

The R&D pursued by the French groups has succeeded to pass almost all the technical hurdles of the PFA-based HCAL. As a result, an HCAL technological prototype with 48 active layers of GRPC, $1m^2$ each was built and successfully operated. The prototype validates the concept of high-granularity gaseous detector and permits to study the energy resolution of hadrons one can obtain with such calorimeter. Four Micromegas of $1m^2$ were also built. They were successfully tested with the previous prototype.

4.1 Readout electronics

The readout electronics of the two Semi-Digital HCAL (SDHCAL) projects were developed in common. An ASIC called HARDROC was first developed to read out the GRPC detectors proposed for the ILD project and then adapted to cope with low-charge signals of the Micromegas detector under the name of MICROROC. To solve the problem of connections related to the high number of electronics channels, the option of a detector embedded electronics using the Daisy chain scheme was chosen and Printed Circuit Board (PCB) were conceived for the readout of large detectors GRPC and Micromegas.

4.1.1 Front-end ASIC

The HARDROC chip (HR) implements a multi-threshold readout which integrates the functionalities of amplification, shaping, digitisation, internal triggering and local storage of the data. Each of its 64 channels consists of a current preamplifier with 8-bit variable gain followed by 3 fast shapers. A low offset discriminator is present on each path and the three corresponding thresholds establish the multi-level readout. A trigger is generated when one of the lowest level discriminators is fired. A frame consists of the 64 encoded discriminator outputs, plus a 24-bit time-stamp and a chip identifier is stored after a trigger is received. Noisy channels could be easily masked via the configuration parameters control. The response of all the channels can be calibrated by injecting an analog signal through an integrated input test capacitor ; this is a useful tool to make the response of the different channels as uniform as possible [33]. The ASIC contains a 127-frame long digital memory. This allows to work in a trigger-less mode and keep all the data accumulated during the bench crossing. An essential feature of the HR is the possibility to be operated in the power-pulsing mode (PP) that consists of switching off almost all power-consumption functionalities in between the bench crossings (BC) of the ILC electron beams. With the ILC duty cycle of one 1 ms of BC every 200 ms, this mode allows a reduction factor of more than 100 of power consumption. Thanks to this reduction, the temperature increase of the HCAL is moderate and only simple cooling system is needed to operate it efficiently. The HR input stage was modified to reach sensitivity to the very small signals generated in the Micromegas (10 fC for a MIP). The modified chip is called MICROROC. Its 64 channels are equipped with a low-noise charge preamplifier (0.25 fC noise) and two slow shapers of 200 ns peaking time to record all the avalanche signal, including the ion tail. The pad-to-pad Micromegas signals have little dispersion (below 10 % RMS) so shaper gain corrections are not necessary. Instead, a DAC was implemented to align the channel pedestals. After alignment a detection threshold of about 1 fC is achieved with channel-to-channel dispersion of 0.1–0.2 fC.

4.1.2 Active Sensor Units

To read out the 1 m^2 detector of the SDHCAL, an electronic board with the same size is needed. This electronic board is an important piece in the present design. It hosts both the pick-up pads and the ASICs in addition to the connections linking the pads to the ASICs and those among the different ASICs. To ensure good transmission qualities and low cross-talk, 8-layer Printed Circuit Board (PCB) is designed. Feasibility constraints did not allow

to have a single board of one square meter. The solution of dividing that circuit into 6 smaller but more manageable PCB was adopted. Each of these small ASUs hosts 24 chips to read out 48×32 pads of 1cm^2 each. This dressed PCB is dubbed Active Sensor Unit (ASU).The routing of each input signal from its own pad up to chip pin has been carefully optimised to reduce the cross-talk. In the case The rooting was conceived so two of the ASUs can be associated to form one slab hosting 48 ASICS. Each slab is then connected to one Detector InterFace board (DIF). The connection between the DIF and the slab as well as the connection of the two ASUs is performed thanks to tiny connectors allowing the different clocks, signals as well as the power to circulate between the two ASUs. Three slabs are then assembled to form the required electronics board with the same grounding reference.

A dedicated PCB was designed for the Micromegas detector. It consists on one side of a matrix of 32×48 copper pads of 1×1 cm^2. On the other side, 24 MICROROC ASICs are soldered. In addition, the pad surface is covered with a Bulk Micromegas. This ASU acts both a signal generating and processing unit. Micromegas

ASU have several special features. They can be connected to each other thanks to small flat connectors, in fact the readout of a chain of 4 ASUs was validated. Routing lines from the ASIC to connectors are dedicated to monitoring the HCAL performance. They can be used to measure the pedestals or inject test pulses to the preamplifiers (ASIC calibration), to read out the shaper outputs for digitisation on an external board (analogue readout) and to measure the temperature on the centre of the ASU.

4.1.3 Front-end and back-end boards

The interface between the ASUs and the data acquisition system (DAQ) is realised by the detector interface board called DIF. The main elements of the DIF is an FPGA and USB, HDMI and SAMTEC connectors. It manages the control signals (*e.g.* clock, busy/ready, external/internal trigger, power-pulsing) and supply power to the ASICs and also performs the readout of the ASIC memories. DIFs are read out by other FPGA-based boards called Data Concentrator Cards (DCC). They can be connected up to 9 DIFs through HDMI links and are controlled by a synchronous DCC (or SDCC). The SDCC can connects to up to 9 DCCs to which it distributes the clock and the commands. It is also connected to the computer network for the user to control the DAQ.

4.1.4 Acquisition software

To exploit the data collected by the SDHCAL detectors an acquisition software was developed. This software is organised in three parts. The first one allows to access the hardware devices (DIF, SDCC) through an FTDI chip associated to each of these devices. It transmits the configurations parameters to ASICs through these devices and collect the data as well. The second part is the configuration data base. It gives the possibility to store and retrieve all parameters needed by the DAQ system. A special care was taken to allow to download the parameters associated to a given parameters of the prototype (roughly 550000 parameters) in few seconds. The third part concerns the data collection. Data from different DIFs may be readout at a different times but will have the same Bench Crossing Identifier (BCID) for a given trigger. The logical way to keep synchronicity is to store in a BCID indexed map the buffers of all read DIFs but it requires to manage memory allocation, access and cleaning. This was achieved thanks to the abilities offered by recent Linux kernels to use file based shared memory. In addition, whenever several computers are involved in the data taking, as it is the case for the SDHCAL prototype, a communication framework is needed. The CMS data acquisition XDAQ framework was chosen. This provides communication tools with both binary and XML, an XML description of the computer and software architecture, a web-server implementation of all data acquisition application and a scalable event builder. A monitoring system was also developed to have a online follow-up of the acquisition during data collection.

4.2 GRPC-SDHCAL

4.2.1 Detector development

The structure of GRPC proposed as an active layer of the HCAL ILD is shown in Figure 10. It is made out of two very thin glass plates.Special spacers were used to maintain uniform gas gap of 1.2 mm. Their number and distribution were optimised to reduce the noise and dead zones ($< 1\%$). The resistive coating on the glass plates which is used to apply the high voltage and thus to create the electric field in the gas volume was found to play important role in the pad multiplicity associated to a mip [33]. To find the best coating for GRPC chambers many products were tested. Finally, a new product based on two components was chosen. By changing the two components ration one can obtain the needed surface resistivity. Another important aspect of this development concerns the gas circulation within the GRPC taking into account that for ILD

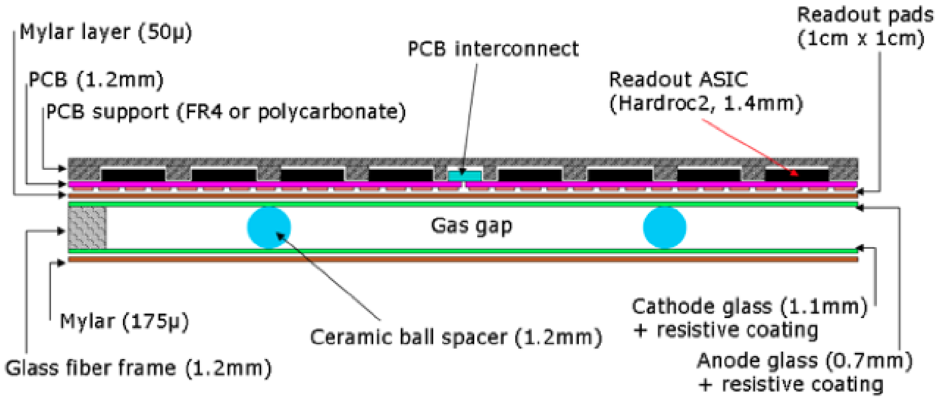

FIGURE 10 – Cross-section through a 1 m^2 chamber.

SDHCAL gas outlets should all be on one side. A genuine system was proposed. It is based on channeling the gas along one side of the chamber and releasing it into the main gas volume at regular intervals. A similar system is used to collect the gas on the opposite side. A finite element model has been established to check the gas distribution [34]. The simulation confirms that the gas speed is reasonably uniform over most of the chamber area.

The GRPC and its associated electronics are housed in a special cassette which protects the chamber and ensures that the readout board is in intimate contact with the anode glass. The cassette is a thin box consisting of 2.5 mm thick stainless steel plates. These plates are also a part of the absorber. The electronics board is fixed on one plate of the cassette. The whole width of the cassette is 11 mm with only 6 of them corresponding to the sensitive medium including the GRPC detector and the readout electronics.

4.2.2 Prototype

A single cassette was first tested in a magnetic field of 3 Tesla (H2 line at CERN) applying the ILC power-pulsed mode [35]. The TB results indicated clearly that the use of the power-pulsed mode in such a magnetic field is possible. The behavior of the detector (efficiency, multiplicity..) was found to be similar to those obtained in the absence of both the magnetic field and the power-pulsed mode (Figure 4.2.3). Following these tests, a technological prototype corresponding to the SDHCAL option proposed in the ILC LOI was constructed (Figure 4.2.3). 48 cassettes as the one described above were built. They fulfilled a stringent quality control. It is worth mentioning that 10500 HR ASICs were produced and tested using a dedicated robot for this purpose. The cassettes were inserted in a self-supporting mechanical structure that was conceived and built in collaboration with the Spanish group of CIEMAT. The structure is made of Stainless Steel plates of 1.5 cm each. The plates were machined to have an excellent flatness and well controlled thickness. In parallel to the prototype construction, in April 2012, the prototype was exposed to pion, muon, electron beams of both the PS and the SPS of CERN. Power-pulsed mode was applied to the whole prototype using the beam cycle structure (0,3 ms time duration for the PS beam and 9 s for the SPS beam every 45 s). A basic water-based cooling system was used to keep under control the temperature increase particularly in in the case of the SPS where the consumption reduction is only 5 (to compare with a factor of more than 100 in the ILC case). An acquisition mode a l'ILC was operated. The data were collected continuously in a trigger-less mode. The DAQ stops when the memory of one ASIC is full. Data are then transferred to a storage station and then the acquisition starts again. Figure 4.2.3 shows the efficiency of the prototype GRPC chambers measured using the muon beam.

The analysis of the the SDHCAL prototype results obtained with a minimum data treatment, shows clearly that excellent linearity and good resolution could be achieved on large energy scale as can be shown in Figs. 4.2.3 and 4.2.3. Furthermore, the high granularity of the SDHCAL provides an excellent tool to thoroughly study the hadronic showers topology and to improve on the energy resolution by separating the electromagnetic and the hadronic contribution. Separation between close-by showers will also get big benefit thanks to the high granularity on the one hand and to to the very clean detector response ($< 1\mathrm{Hz/cm}^2$) on the other hand. These different points are being worked out and preliminary results confirm the expectations.

The quality of data obtained during four weeks of beam tests validates completely the SDHCAL concept as proposed in the LOI. This is especially encouraging since no gain correction was applied to the electronics channels to equalise their response. Gain correction mode has been elaborated recently and will be tested in the future beam tests.

4.2.3 ILD Preparation

The knowledge acquired with the construction, the commissioning and the results of the technological prototype were used to implement a realistic simulation of the ILD HCAL. Physics channels such as the $t\bar{t}H$ were studied using the SDHCAL option and results were found identical to those obtained with the scintillator tile option despite the fact that the jet energy reconstruction code was optimised for the latter.

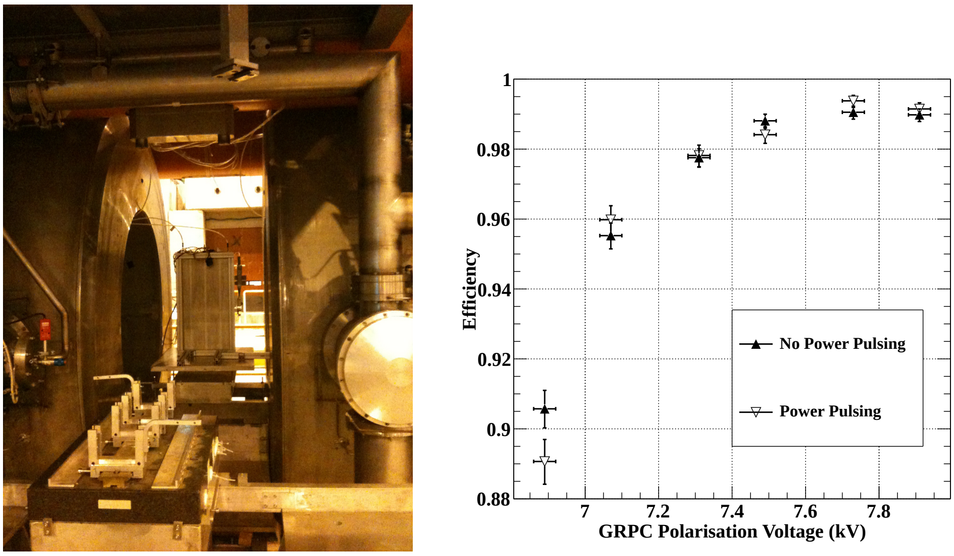

FIGURE 11 – GRPC setup in the CERN SPS-H2 line magnetic field(left).Efficiency scan over high voltage, with and without power pulsing(right).

4.3 MICROMEGAS-SDHCAL

Micromegas have a linear response and are therefore well suited for sampling calorimetry. They are studied for the SDHCAL of a future linear collider experiment [36]. Technologically advanced prototypes were built. They are equipped with an electronics similar to RPCs so combined testbeams could be conducted. The Micromegas group is also active in simulation of the SDHCAL performance and participate to the analysis effort of the RPC-SDHCAL testbeam data. The group also proposed an engineering solution for the barrel

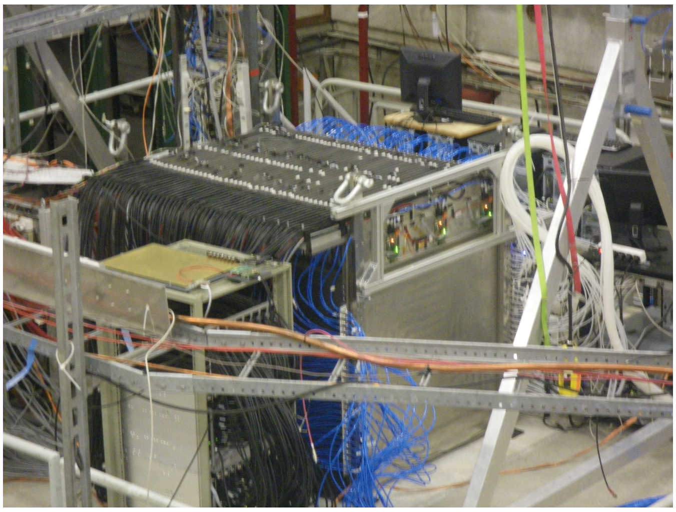

FIGURE 12 – SDHCAL-GRPC prototype.

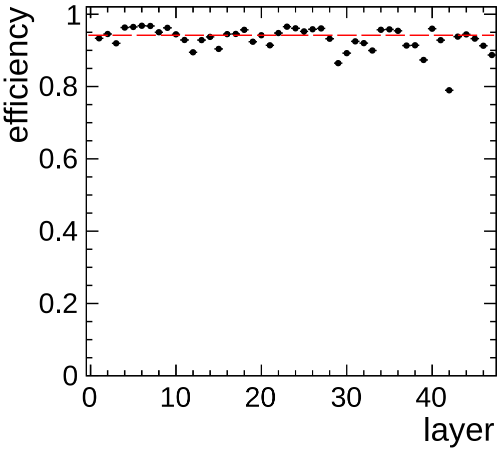

FIGURE 13 – Efficiency of the SDHCAL-GRPC prototype.

mechanics of the SiD detector concept. In this section, only prototyping work and testbeam results are emphasised.

Chamber mechanics The $1{\times}1\,\mathrm{m}^2$ Micromegas prototype is formed by 6 ASUs glued to a thin vetronite mask. The outer edges of the ASUs are surrounded by a square plastic frame. The chamber is closed by a steel cover on which a thin drift electrode is printed. This cover is glued to the frame. To avoid bending of the cover and change of the gas gap, 3 mm thick spacers are inserted in the 1 mm gap between ASUs. Readout boards and patch panel for services are fixed to the cover. With this design, a chamber thickness of ~ 1 cm is achieved with dead zones of 2 %.

Operating facts The operating gas gain is quite low ($\sim 2{\times}10^3$) and easily achieved in argon-based mixtures. $\mathrm{Ar}/i\mathrm{C_4H_{10}}$ was used until 2013 when stable operation in $\mathrm{Ar/CO_2}$ (a non-toxic and non-flammable mixture) was demonstrated. Bias voltages remain below 1 kV and detector currents at the level of a few nA. During testbeam of the SDHCAL, a signal-to-noise ratio of 20 is achieved. This allows to set the channel threshold at ~ 1 fC. At this threshold, the fake hit rate (or noise rate) per chamber is ~ 200 Hz and the fraction of masked channels is ~ 0.2 %.

MIP characterisation A high MIP efficiency is achieved at low gas gain as expected from the low readout threshold. It is illustrated by the red line in Figure 16 (left). Also, the efficiency shows little spread : at a given threshold, it is similar in all chambers (Figure 16 (left)) and the dispersion over the $1\,\mathrm{m}^2$ area of each chamber is of a few percents. This excellent uniformity implies that the calibration of a Micromegas sampling calorimeter should be simple. All layers having the same response to MIPs (and probably to showers too), there is no need for position-dependent weights when measuring shower energies. Therefore the constant term of this calorimeter should be small (and its noise term negligible).

Behaviour in hadron showers Sparks and rate effects can induce dead time and inefficiency loss which in a calorimeter would manifest as a saturated response and a worse energy resolution. They were studied in a 150 GeV/c pion beam using a setup of four prototypes placed downstream a $2\,\lambda_{\mathrm{int}}$ thick absorber block. Most

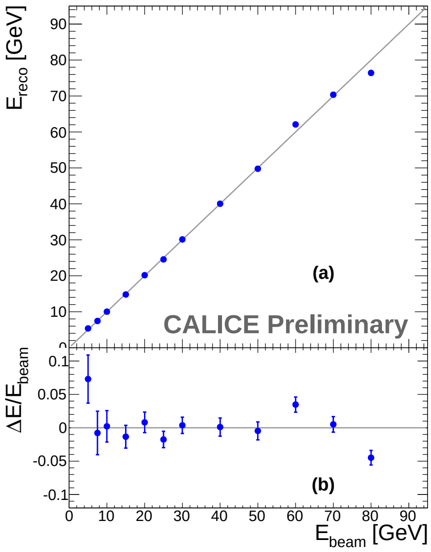

FIGURE 14 – (a) : Mean reconstructed energy for pion showers and (b) : relative deviation of the pion mean reconstructed energy with respect to the beam energy.

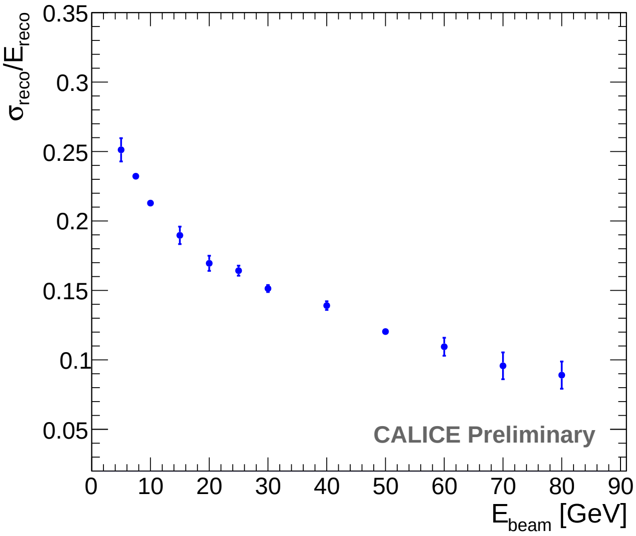

FIGURE 15 – $\frac{\sigma_{reco}}{E_{reco}}$ of the reconstructed pion energy E_{reco} as a function of the beam energy.

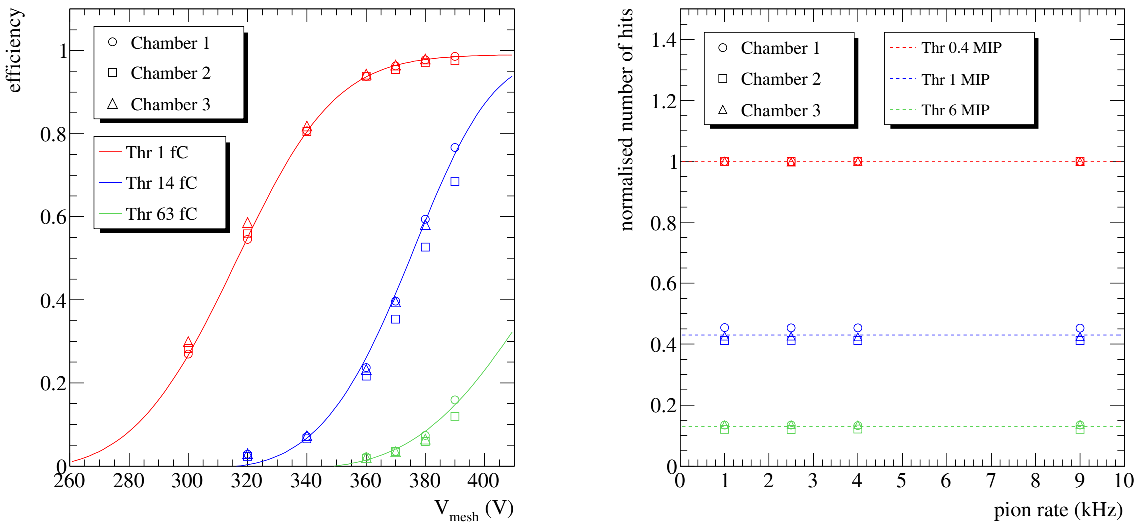

FIGURE 16 – Efficiency to 150 GeV muons versus mesh voltage in 3 $1{\times}1\,\mathrm{m}^2$ Micromegas prototypes (left). Normalised response of 3 prototypes to 150 GeV pions behind 2 λ_{int} or iron (right).

pions shower inside the absorber and the shower remnant is measured with the prototypes. The distribution of the number of hits was measured for pion rates up to 10 kHz. It has a mean value of 60 hits and an exponential-like tail up to 300 hits. At three values of threshold, the distribution is independent of rate (Figure 16 (right)).

Sparks are identified with the HV slow-control system as sudden current peaks flowing through the gas from mesh to ground. Per $1\times1\,\mathrm{m}^2$ chamber, a spark probability between 1–5×10^{-6} is found. This is probably sufficiently low for a 50 layers SDHCAL in ILC-like conditions. Alternative Micromegas designs, however, are investigated to fully suppress sparks (section 4.3).

Response of a virtual Micromegas SDHCAL Thanks to the common DAQ developed for the SDHCAL by IN2P3 groups, combined tests with 46 RPCs and 4 Micromegas were conducted. This provided the opportunity to indirectly measure the pion response (*i.e.* $N_{\mathrm{hit}}(E_{\mathrm{beam}})$) of a fully equipped (hence virtual) Micromegas SDHCAL. The measurement is performed in 2 steps. The longitudinal shower profile is first measured (in the Micromegas layers) at several pion energies by exploiting the large fluctuations of the starting point of hadron showers. Secondly, the profile is integrated from zero to infinity, yielding the average number of hits that would be measured in an infinitely deep Micromegas SDHCAL. The profile is shown in Figure 17 (left) for pion energies of 20–150 GeV. The response is plotted next to it, together with the predictions of a Monte Carlo simulation. It is in agreement with the one of the RPC-SDHCAL up to a scaling factor corresponding to the single particle hit multiplicity. The saturation is observed but can be corrected using the information from additional readout thresholds. This off-line compensation technique was developed with Monte Carlo simulation and proved to work on RPC testbeam data.

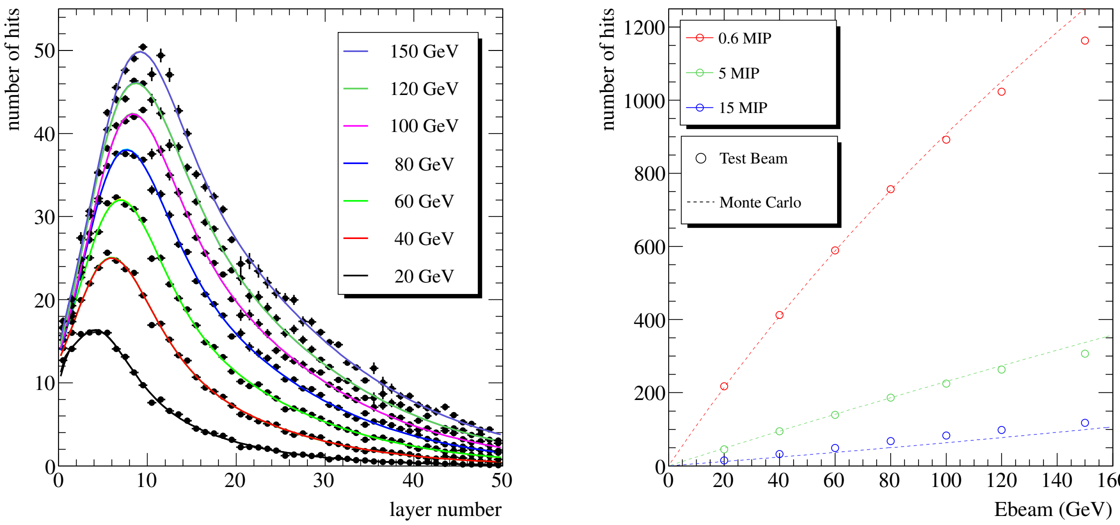

FIGURE 17 – Profile of pion showers measured in the Micromegas layers of the SDHCAL (left). Pion response of a virtual Micromegas SDHCAL obtained by integration of the profile (right).

Spark suppression in resistive Micromegas Although rare, sparks between mesh and anode pads can damage the front-end electronics. For this reason, current-limiting diodes are soldered on the ASUs of the $1\times1\,\mathrm{m}^2$ prototypes, between pads and ASIC inputs. This protection scheme has been so far successful but involves many passive components. It is therefore not cost-effective for mass production. Resistive coatings on the detector electrodes slow down the evacuation of charge which reduces the applied electric field. By this mechanism, they efficiently quench sparks upon ignition but at the expense of rate capability and linearity as the field is restored after a certain time constant. Resistive and non-resistive ASUs of $16\times16\,\mathrm{cm}^2$ were tested in beam in 2013. Resistive configurations fully suppress sparks and the resulting voltage drops normally observed in non-resistive ASUs (Figure 18). Rate scans were performed with electrons up to $50\,\mathrm{kHz/cm}^2$. They indicate stable performance up to $10\,\mathrm{kHz/cm}^2$ and a few percent efficiency loss above.

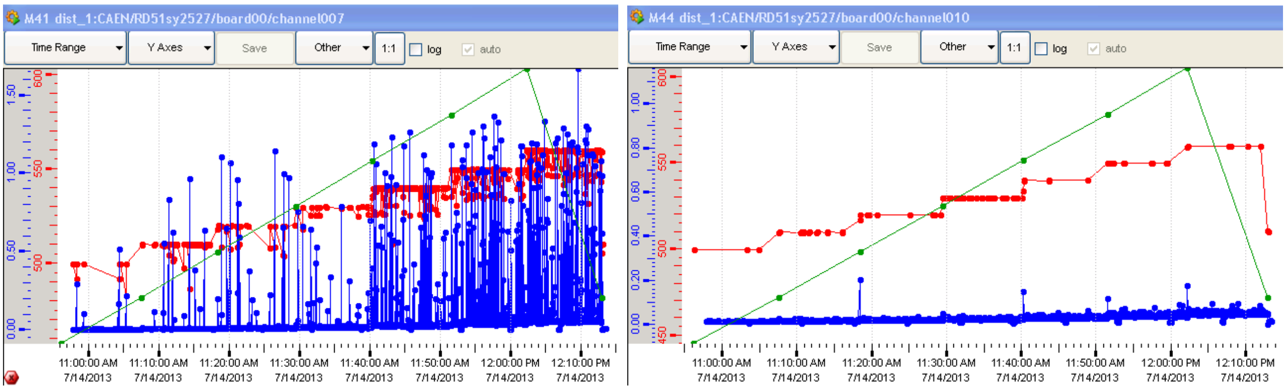

FIGURE 18 – Measured mesh current (blue dots) when ramping up the voltage (red dots) of non-resistive (left) and resistive (right) Micromegas in a 1 kHz electron beam.

4.4 SDHCAL Future R&D

4.4.1 GRPC

Large GRPC of $1\mathrm{m}^2$ were developed and built for the technological prototype. However, larger GRPC are needed in the future DHCAL with the largest one being 290X91 cm2. These large chambers with gas inlet and outlet on one side need a dedicated study to guarantee a uniform gas gap everywhere notwithstanding the angle of the plate. It is necessary also to ensure an efficient gas distribution as it was done for the 1 m2 chambers. To improve on the prototype readout electronics performances a new version of the HARDROC ASIC allowing larger dynamic range was conceived, produced and tested successfully. The new ASIC allows to be directly addressed and easily bypassed in case of failure. We intend to use the new ASICs to read few large GRPC chambers $> 2\mathrm{m}^2$). In addition, we intend to improve on the interface boards (DIF) needed to control the ASICs synchronisation and data transfer. Indeed, the space left between the active layer of one module and the cryostat is only 5 cm. This means that the DIF components should be optimised to cope with the volume availability.

4.4.2 MICROMEGAS

Two R&D phases were emphasised : the construction of large area Micromegas and of small resistive Micromegas. Both were successful, part of the results were published [37] and two papers are about to be submitted. The next phase is naturally the construction of an advanced calorimeter prototype instrumented with resistive Micromegas (of smaller lateral size than the current SDHCAL prototype). This ambitious project is relevant to a linear collider detector but also to higher rate applications (*e.g.* HL-LHC upgrades). It is highly constrained by funds and a proposal has been submitted to the ANR agency. If accepted, it will probably cover the 2015-2017 period. Independently of the proposal outcome, 2014-2015 will be dedicated to the design, fabrication and test of $50{\times}50\,\mathrm{cm}^2$ resistive ASUs. These ASUs are necessary to validate the concept of large area resistive Micromegas. They would also be the basic unit of the proposed calorimeter.

5 INTEGRATION & COSTS STUDIES FOR ILD

The information described here is essentially taken from the detector parts of the TDR. The reader is referred to them for details ; only key elements need for the understanding of the IN2P3 contributions are mentioned.

The integration of the different sub-detectors into a coherent and functioning detector concept is critical for the final performances. This is even more true for Particle Flow oriented detectors using a fine interplay of each detector performances ; results in beam test from detectors have to be folded in the complete detector and the touchstone for physics performance is the Jet Energy Response rather than the "standard" single particle response. The mechanical integration, but also the coordination of the services, cabling, cooling strategies, thermal stabilisation and alignment of the various sub-detectors as well as the mounting procedures are continuous tasks, following the respective detector technologies. The envisaged push-pull scenario at the ILC imposes additional requirements (stability, stray magnetic field) and costs. If the final level of achievement of technology and production of sub-detector might vary (roughly from the outer/bigger to the inner/smaller) the global design should be fixed first, that is as soon as the construction is decided (as early as 2016 in the fast-track scenario).

The IN2P3, and especially the LLR, have had contributions in the global design of ILD – and to a lesser extend the Experimental Hall design – in the precision of the push-pull constraints on the detector, as well as the mechanical simulations of deformation of the coil under its own weight and in response response to seismic vibrations [38].

The ILD conception, mechanical modelling and studies, as well as the detailed GEANT descriptions were performed on the ECAL barrel (LLR), endcaps (LPSC), HCAL (IPNL, LLR). The models were merged in global ones, for mechanical and for simulation (both developed and maintained at LAL and LLR). The mounting and parametric cost aggregation of the sub-detector as well as the estimation and modelling of the services volumes were done at LLR.

Additionally, but not further detailed here : the SiD HCAL structure design, mechanical stability and effect on physics reconstruction was realised in LAPP. It is described in the SiD LoI [7].

5.1 ILD Modelling

Three different types of models are being used for the design of the ILD detector. The general placeholder describing boundaries and volumes of the sub-elements, assembling spaces and tolerances, used for fast integration, checks for conflicts and compliance of the interfacing components was developed and maintained first at LLR, then at LAL.

Detailed engineering models of the sub-detectors were the responsibilities of IN2P3 groups for the HCAL and ECALs. They define how to assemble a component from parts, provide exact geometry and material description and were used as the basis of the cost evaluations.

The same sharing of responsibility was true for the Physics simulation models describing the segmentation, shape, and physics behaviour of the active and passive components for each sub-detectors. The ILD physics model is based on the GEANT4 full detector with an parametric geometry overlay, allowing for virtually any scaling comparison, MOKKA [39] developed and maintained at LLR. MOKKA has also been used for the modelling of most of the CALICE test beam set-ups. In the framework of AIDA, it will be adapted to new geometry package dubbed DD4HEP [40].

5.2 Design

HCAL design : The French groups participated actively in the HCAL part of the ILC TDR (ILD part) by proposing a genuine mechanical structure for the hadronic calorimeter barrel (called V-structure [4]) resembling the one of H1. The V-structure features five rings, assembled from eight wedge-shaped modules each. It was conceived to eliminate the projective holes and cracks so none of the particles produced close to the detector centre could escape detection. It minimises (but for safety margin) the space between the barrel and the end-caps avoiding dead space [5] In this structure the HCAL barrel services such as the gas tubes, data collection and electric cables are deported to the outer radius.

The barrels are supported from rails in the cryostat. The mass of the HCAL steel absorber structures is of the order of 600 t. Detailed mechanical studies have shown that the expected deformation are only in the order of a few millimetres.

On site monitoring of the deformation is something that is "easily" achievable by the use of Fibre Bragg Grating, by embedding sensible fibres in the structures. This is foreseen for the ECAL Carbon Fibre structure (equipped), and is seen as a key future technique to be managed at the IN2P3 [6].

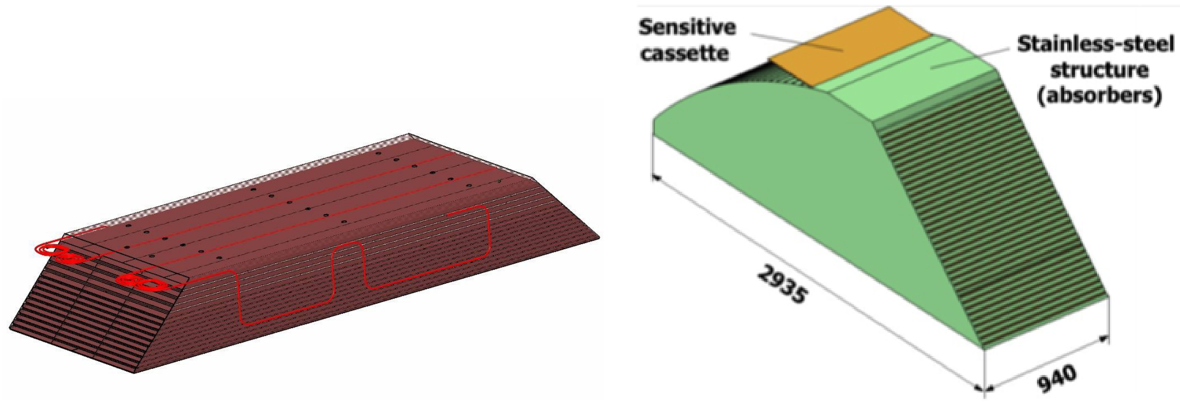

FIGURE 19 – Left) Embedding of fibres in the ECAL CF structure for structural monitoring of distortion, temperature, humidity, etc. ; Right) One module of the SDHCAL barrel.

ECAL Barrel : The electromagnetic calorimeter (ECAL) modules are supported by low Z (aluminium or carbon) rails from the HCAL barrel modules. Figure 22 shows the installation procedure of the ECAL modules with the use of an external cradle that holds a rotatable support cage will be used during the installation phase. The cost of such equipment was taken into account as much as possible in the estimations.

The Tungsten-Carbon fibre mechanical structure of the barrel modules was designed from the start to ensure mechanical rigidity, self-support and industrialisation. The dimensions of every element is optimised w.r.t the largest size of Silicon wafers (to lower its cost), the reduction of dead spaces (for optimal shower compactness).

ECAL Endcaps : The endcap calorimeters are supported from the endcap iron yoke. The support for the HCAL endcap from the yoke needs to balance the bending of the iron yoke in the strong magnetic field.

4. in reference to his promoter, H. Videau

5. in the alternative design, CMS- and TESLA-like [41], electronics and services occupy this space (see fig 21).

6. FBG monitoring is applicable to many other detectors (TPC, Vertex) ; it is being now tested in AIDA for Belle VTX detector.

Magnetic and mechanical calculations were performed to ensure sufficient margin for the deformation of the yoke endcaps under the magnetic field for a residual field safe for work in proximity (mandatory in case of push-pull).

The final design of the ECAL endcaps, using similar structure as for the barrel but with a longer range, still requires some work as it was recently noticed that the mechanical stress is slightly too high.

Beampipe & Inner tracking system : The inner tracking system consists of the Silicon Inner Tracker (SIT), the Forward Tracking Disks (FTD) and the Vertex Detector (VTX). These detectors will be mounted together with the Beryllium beam pipe in the Inner Support Structure (ISS), as indicated in figure 20. As the push-pull system will align the overall ILD detector axis only to ±1 mm, a re-adjustment of the beam pipe might be necessary to keep the stay-clear margin between the beam pipe and the cone of background radiation at safe levels. Details of the inner detector system are described in [42].

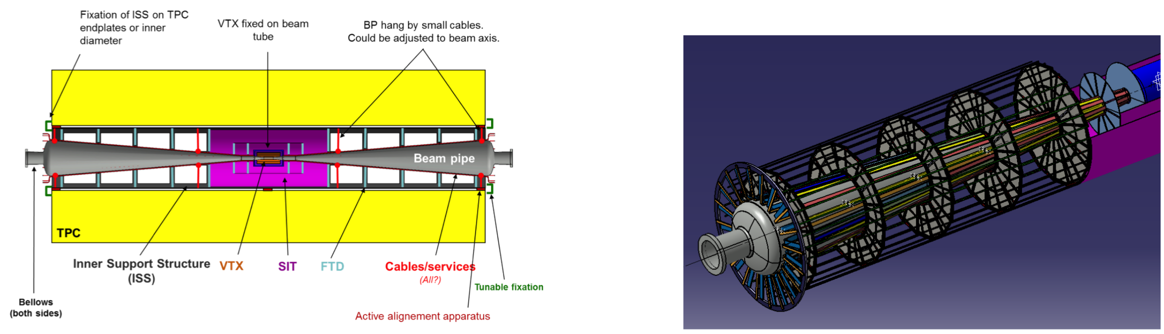

FIGURE 20 – Left : support of the inner tracking detectors. Right : schematic representation of the cable distribution along the beam pipe (from IP to the position of TPC endplate).

Further studies will have to be performed to ensure that vibrations stemming from the 5 Hz power pulsing in the strong magnetic field stay at a reasonable level. The same stay true for push-pull operations. Finally although challenging a complete thermal study of the detector to ensure that each component stats in a working range, will have to be performed.

Services, Paths, Interfaces and Acquisition : A number of services (cables, cooling, gases) are needed for the operation of the ILD detector, reduced to a minimum thanks to the utilisation of power-pulsing and local zero-suppression and storage. The total section of the power and readout cables, and cooling pipes has been estimated by each sub-detector. The information was centralised and implemented : the path and position of patch panel and power converters optimised to reduce the mount of dead materials and ease of mounting Figure 21. The corresponding materials were then modelled in the description of the detector used the simulation for the DBD performance estimation [43, 44] (Figure 21 right)

A special effort was needed for the cable layout of the inner detector silicon (VTX, FTD, SIT) as they represent dead material immediately around the beam pipe and may become a source of background. Specific R&D on the definition of the cables according to the nature of the conductor and the optimisation of the insulator is mandatory in order to minimise the effects of the services on the physics performance of the detector. A schematic view of the cable routing in the inner detector is shown in figure 20.

Last, but not least, the acquisition system (DAQ) for the calorimeters has been designed following the solutions designed for SDHCAL and ECAL. The update of the acquisition system requirements for the DBD was done at LLR, in view of the gained experience from the calorimeter test beams and from the common

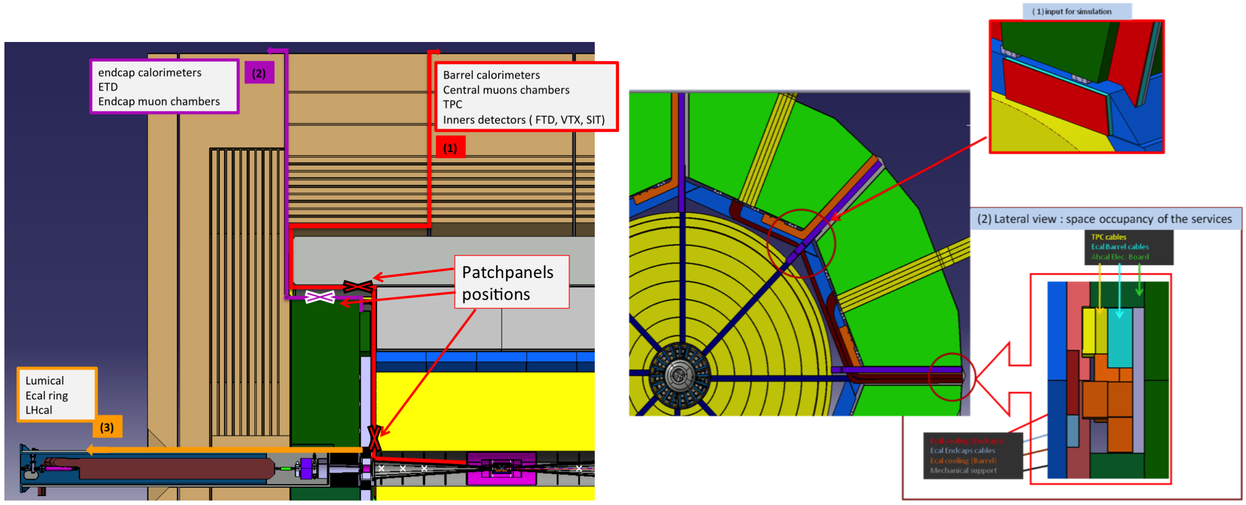

FIGURE 21 – Left) Illustration of the main service paths in the ILD detector (here for the HCAL TESLA design). Right) Front view of the barrel calorimeters (green/blue), TPC (yellow), inner part and of their associated services. (1) The volume occupied by cables and services in each way-out has been translated into equivalent thickness of conductor and insulator to be implemented in the simulation model. (2) Lateral view of one way-out, with representation of the space needed per sub-detectors services.

DAQ (i.e. with trackers) effort in the framework of AIDA. A complete "slice test" involving an element of each ILD sub-detectors is one of the collaboration building path foreseen to be pursued in an H2020 program.

5.3 Detector assembly

The detector assembly was studied for two cases : non-mountainous sites, and mountainous sites. In the first case, the assembly would be similar to the CMS one, with a pre-assembled sections levered down a large access shaft. Space need for the movement of the various pieces, mostly on air-pad, and maintenance operations has been estimated, for the case of a push-pull solution.

In the case of a mountain site, as now foreseen, the access is provided by a km long tunnel limiting the size of the elements in transit ; the largest one being the coil. The yoke would be assembled in the hall. The procedure influences the total cost of the cavern and needs to refined, especially in view of a reduction of the radius of the detector w.r.t. the current design.

HCAL rings, rotated and inserted using a bed [45].

5.4 Re-optimisation of ILD

Since the fusion of the LDC (European) and GLD (Japanese) detector concepts into ILD some key parameters, such as the radius of the TPC and the half length of the barrel, have been fixed on average values ; this was used for the LoI and the DBD. In view of increased SW performances (especially in PandoraPFA) and ECAL and SDHCAL granularities, it has been recently shown [27] that a decrease of the TPC radius and half length by 30 %, would impact the Jet Energy Resolution quite mildly (10 %) for a gain on the nearly a factor 2 on the external and most expensive elements of ILD : ECAL, HCAL, Coil and Yoke. The reduction of the coil radius would also decrease the price of the access tunnel and of the cavern in amounts yet to be estimated.

The study has to be continued and extended around a new set of reference parameters to check the effect

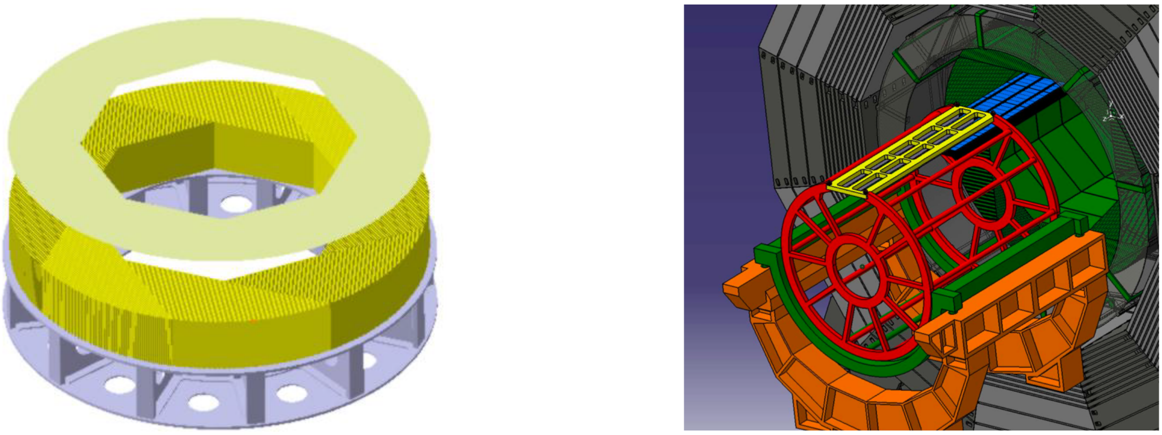

FIGURE 22 – HCAL and ECAL installation.

of combined reduction of layers in the SiW ECAL, eventually a possible hybridisation with scintillators strip solution proposed by the Japanese ECAL group. The effect on special channels (especially Tau reconstruction) whose performance is not driven by JER has also to be assessed.

Finally, these studies should be made in view of the large but somehow uncoordinated French efforts in the development of innovative Particle Flow techniques[7] using the unprecedented level of details offered by imaging calorimeters. A specific ANR support was requested this year on this topic. Currently the most performing PFA tool (PandoraPFA) used for the LoI and DBD studies has been developed – and optimised – by UK and German colleagues on options not necessarily ideal for the French community.

7. These include e.g. tracks and tree reconstruction in calorimeters, high performance photon tagging in jets, self-learning shower classifications...

6 SUMMARY AND OUTLOOK

Intense and steady detector oriented activities are carried on in IN2P3 laboratories since many years in perspective of the construction of the ILC. This document provides an overview of these activities, focusing on the last 5-6 years. Most of them resulted into prominent contributions to the DBD, which accompanies the ILC TDR, a culminating point resulting from a machine design effort over nearly twenty years of R&D.

The TDR provides a detailed description of the machine design, complemented with well advanced designs of two detector concepts developed within large international teams. Besides substantial efforts invested in the machine R&D and beam instrumentation, out of the scope of this document, several tens of IN2P3 physicists, engineers and PhD students (15 theses completed since 2008 and 9 theses that are ongoing) have been very actively developing solutions adapted to the challenges inherent to the required highly granular and low power detector, based on a very light, high precision, tracking system.

Several of these activities were accompanied by physics performance studies which guided the trade-off to be found between conflicting detector requirements, and were complemented with detailed, highly realistic, studies of detector integration and costing.

Original technical solutions were found and proposed by these groups, which have substantially contributed to demonstrate the feasibility of a detector taking optimal advantage of the experimental sensitivity accessible at the ILC. Because of its essential contributions, the IN2P3 community has been acknowledged for its expertise, strength, reactivity and achievements, as well as for the substantial resources that have been attributed to realise its diversified R&D programme.

The R&D on vertex detectors has generated substantial progress on the detection elements as well as on the system integration and the overall detector concept. As a major outcome, a new position sensitive technology has been established, which is getting used in a growing number of applications, including LHC experiments. For the ILC, it is the pixel technology offering the highest potential among all technologies actively developed today. It is particularly attractive for achieving bunch tagging, a prominent goal of the R&D in the coming years. The possibility to integrate $50\,\mu m$ thin CPS in ultra-light double-sided pixelated ladders has been demonstrated, with a perspective of less than 0.3 % X_0 material budget. Achieving this challenging material budget performance is among the major goals of the coming years' R&D, as well as validating the concept of spatial resolution associated to time-stamping via impact correlations from both ladder sides. These tasks will be accompanied with a study of ladder power pulsing in a high magnetic field. Finally, a vertex detector concept has been designed, based on CPS, which is presently the best adapted to the beam related background among all options under development. An alternative, delayed read-out, approach using fine pixels may also be investigated in the coming years, which would provide improved spatial resolution and avoid the delicate operation of power pulsing.

For the electromagnetic calorimeter the focus will be on two aspects. These are a stack of fully equipped ASUs and at least one long layer with up to 10 ASUs. If enough manpower is available the work on this can be parallelised. It is envisaged to go to beam test at CERN with a calorimeter stack that comprises between 20 and 30 (short) layers. The beam test campaigns should start during 2015. Successful beam test campaigns in the years 2015-2016 require as well the production of a version 2b of the SKIROC ASIC. It is essential that this ASIC gets characterised as quickly as possible to prepare for the version SKIROC3 that is supposed to work in an ILC detector. The entire R&D has always taken into account aspects on the industrialisation of the detector construction to be ready in case of a positive decision on the ILC.

Concerning the hadronic calorimeters, the exploitation of beam tests data of the SDHCAL prototype, which was the first technological prototype to be built and operated, will be the major activity in the two coming years. In parallel, and in order to completely validate the concept of the SDHCAL, the development of large gaseous detectors such those foreseen in the future ILC experiments, will be pursued. A new version of the read-out electronics solving the few remaining problems encountered in the technological prototype, needs also to be completed and tested on large detectors. Technological aspects related to the integration of the SDHCAL must also be addressed.

In the last three years, important progress was achieved with the Micromegas option for the SDHCAL. The R&D work now focuses on improving the spark protection scheme with resistive coatings. To ultimately assess the benefits of a Micromegas calorimetry, however, a few tens of layers are needed. A calorimeter prototype instrumented with small size resistive Micromegas layers is necessary. Its construction and test could be completed before 2018 while waiting for a decision from Japan to host the ILC. In case of a positive decision, a choice of technology for the SDHCAL will be made which justifies the realisation of a Micromegas calorimeter.

Besides the contributions concentrating on the ILC project, the detector R&D has generated numerous spin-offs which often address less demanding applications than ILC. For instance, the pioneering development of CPS has ended up with a world-wide used high-precision beam telescope [46] (realised within the EUDET project) and with the first use of such sensors in several tracking devices equipping heavy ion collision experiments (STAR [12], ALICE [13, 14], CBM [47], ...) as well as in research equipment for hadrontherapy (FIRST experiment, GSI, ...).

Detectors similar to the electromagnetic calorimeter physical prototype described above have been constructed (for the PAMELA satellite [48], the PHENIX NoseCone calorimeter [49]) and are envisaged for several other experimenents (CHIC, CMS endcaps). As can be already concluded from this document the 'ROC' ASICs are applicable to all types of highly granular calorimeters. Variants of this type of ASIC are used in Space Research but also in Earth Sciences and Medical Applications. Data of highly granular calorimeters are an ideal testing ground for pattern recognition algorithms, in particular those of a new discipline called deep learning considered to revolutionise machine learning in the coming years.

The development of gaseous detectors and their electronics read-out as active media for the hadronic calorimeters by the French groups, allowed for acquiring a good and recognised expertise. The TOMUVOL project, which aims at studying the volcano structure, is using GRPC that are similar to those developed for the SDHCAL. Another variant of the same detector using doped glass and standing high detection rate was proposed to equip the muon detectors of the high η region of CMS. It is considered as one of the two principal technologies to be examined by the CMS collaboration for the CMS-update.

The high level of expertise acquired by the IN2P3 groups will turn into an important asset once the ILC project gets approved, if so. Several considerations (resources, time, availability of scientists' community, ...) tend to make it questionable whether there will be two detectors right at the beginning of the ILC operation. If there would be only one, the question of its concept (semi-conducting or gaseous main tracker, more or less compact design) remains open today. It may therefore be justified to keep an expertise variety and a position of acknowledged source of proposal for the discussions expected in the coming 2-3 years, and thus be one of the driving actors of the emergence of a detector concept accommodating the forthcoming scientific, economic and political context. Whatever the concept retained will be, a diversified and solid know-how will settle the IN2P3 community in a situation favourable to its interests.

This community has however shrunk substantially in the last couple of years, and is presently more than two times smaller than it used to be a few years ago. This trend has become a concern at a time when the Japanese side is watching the strength of the ILC community of each country and tends to interpret it as an expression of scientific interest for ILC. During the coming 2-3 years, while discussions about ILC will be going on between Japan and countries expected to participate to the machine and detector construction, it is essential that the IN2P3 community remains well involved and supported. Emerging EU programmes are examined with much attention in the perspective of being a relevant funding source for pursuing R&D activities towards their ending result.

If a positive decision on the ILC emerges until 2015-2016, the IN2P3 groups intend to join the world wide effort of finalising the engineering prototypes of the calorimeters, choosing their technologies and finetuning their concepts. 2-3 years are expected to be necessary for this step. Meanwhile, the community will continue examining how to concentrate its forces on the construction of one of the calorimeters. However, there are pending issues, such as the number of detectors (1 or 2) and the potential reinforcement of the IN2P3 community consecutive to the machine construction approval, which may have a strong impact on this choice, and need therefore to be cleared out prior to a decision. Meanwhile, it is important to maintain the present diversity of know-how, which will enhance the capability of the IN2P3 groups to adapt to a variety of possible evolutions of the detector design.

Contrary to the calorimeters, which may typically start construction around 2020, the vertex detector is expected to start construction several years later and should thus benefit from further evolutions of industrial technologies. It would therefore be possible for IPHC to complete the sensor R&D and contribute to the technical choices to be made in the next decade. The possibility to contribute to the construction of the vertex detector itself (among the least expensive sub-systems) is therefore unlikely to become a subject of debate before 10-12 years, in a context which has presently many unknowns, the sensor technology being among the most prominent ones.

Concluding, the IN2P3 community involved in the ILC project is eagerly awaiting the decision for the machine to be built in Japan. While waiting for this decision to be taken in the coming 2-3 years, it is determined to continue its major R&D activities within a well defined programme, despite the restricted financial short- or mid-term perspectives and modest remaining human resources. It is also well prepared for the debate on the finalisation of the detector designs, and is getting prepared for the choice of the sub-systems it could contribute constructing. These instrumental activities need to be pursued in parallel with studies preparing the physics program, relying in particular on PhD students, for which funding possibilities will be investigated (including EU programs and shared tutoring frameworks). The aforementioned period is perceived by the groups as critical for their future. In case a positive decision would not emerge in the upcoming 2-3 years, the groups would fully revisit their plans and start considering alternative projects.

Références

[1] B. Barish and J. E. Brau, "The International Linear Collider" *Int.J.Mod.Phys.* **A28** (2013) no. 27, 1330039, arXiv:1311.3397 [physics.acc-ph].

[2] C. Adolphsen, M. Barone, B. Barish, K. Buesser, P. Burrows, *et al.*, "The International Linear Collider Technical Design Report - Volume 3.II : Accelerator Baseline Design" arXiv:1306.6328 [physics.acc-ph].

[3] M. Altarelli, R. Brinkmann, M. Chergui, W. Decking, B. Dobson, *et al.*, "XFEL : The European X-Ray Free-Electron Laser. Technical design report".

[4] T. Behnke, J. E. Brau, P. N. Burrows, J. Fuster, M. Peskin, *et al.*, "The International Linear Collider Technical Design Report - Volume 4 : Detectors" arXiv:1306.6329 [physics.ins-det].

[5] D. Asner, T. Barklow, C. Calancha, K. Fujii, N. Graf, *et al.*, "ILC Higgs White Paper" arXiv:1310.0763 [hep-ph].

[6] **ILD Concept Group - Linear Collider Collaboration**, T. Abe *et al.*, "The International Large Detector : Letter of Intent" arXiv:1006.3396 [hep-ex].

[7] H. Aihara, P. Burrows, M. Oreglia, E. Berger, V. Guarino, *et al.*, "SiD Letter of Intent" arXiv:0911.0006 [physics.ins-det].

[8] "Web site of PICSEL group of IPHC". http://www.iphc.cnrs.fr/-PICSEL-.html.

[9] M. Battaglia, C. Da Via, D. Bortoletto, R. Brenner, M. Campbell, *et al.*, "R&D Paths of Pixel Detectors for Vertex Tracking and Radiation Imaging" *Nucl.Instrum.Meth.* **A716** (2013) 29–45, arXiv:1208.0251 [physics.ins-det].

[10] C. Hu-Guo, J. Baudot, G. Bertolone, A. Besson, A. Brogna, *et al.*, "First reticule size MAPS with digital output and integrated zero suppression for the EUDET-JRA1 beam telescope" *Nucl.Instrum.Meth.* **A623** (2010) 480–482.

[11] I. Valin, C. Hu-Guo, J. Baudot, G. Bertolone, A. Besson, *et al.*, "A reticle size CMOS pixel sensor dedicated to the STAR HFT" *JINST* **7** (2012) C01102.

[12] L. Greiner, E. Anderssen, H. Matis, H. Ritter, J. Schambach, *et al.*, "A MAPS based vertex detector for the STAR experiment at RHIC" *Nucl.Instrum.Meth.* **A650** (2011) 68–72.

[13] J. Baudot, A. Besson, G. Claus, W. Dulinski, A. Dorokhov, *et al.*, "Optimisation of CMOS pixel sensors for high performance vertexing and tracking" *Nucl.Instrum.Meth.* **A** (2013) no. 732, 480, arXiv:1305.0531 [physics.ins-det].

[14] **ALICE Collaboration**, L. Musa *et al.*, "Upgrade of the ALICE Inner Tracking System" *CERN-LHCC-2013-024 ; ALICE-TDR-017* (2013) . https://cds.cern.ch/record/1625842?ln=fr.

[15] **PLUME Collaboration**, A. Nomerotski *et al.*, "PLUME collaboration : Ultra-light ladders for linear collider vertex detector" *Nucl.Instrum.Meth.* **A650** (2011) 208–212.

[16] **CALICE Collaboration**, J. Repond *et al.*, "Design and Electronics Commissioning of the Physics Prototype of a Si-W Electromagnetic Calorimeter for the International Linear Collider" *JINST* **3** (2008) P08001, arXiv:0805.4833 [physics.ins-det].

[17] **SiW Ecal group within CALICE**, M. Anduze *et al.*, "JRA3 Electromagnetic Calorimeter Technical Design Report". http://www.eudet.org/e26/e26/e27/e43691/eudet-report-09-01.pdf. EUDET-Report-2009-01.

[18] R. Pöschl and the CALICE Collaboration, "R&D for a SiW Electromagnetic Calorimeter for a Future Linear Collider" *Journal of Physics : Conference Series* **293** (2011) no. 1, 012069. http://stacks.iop.org/1742-6596/293/i=1/a=012069.

[19] **CALICE Collaboration**, C. Adloff *et al.*, "Effects of high-energy particle showers on the embedded front-end electronics of an electromagnetic calorimeter for a future lepton collider" *Nucl.Instrum.Meth.* **A654** (2011) 97–109, arXiv:1102.3454 [physics.ins-det].

[20] **CALICE Collaboration**, R. Cornat, "Semiconductor sensors for the CALICE SiW EMC and study of the cross-talk between guard rings and pixels in the CALICE SiW prototype" *J.Phys.Conf.Ser.* **160** (2009) 012067.

[21] S. Callier, F. Dulucq, C. de La Taille, G. Martin-Chassard, and N. Seguin-Moreau, "SKIROC2, front end chip designed to readout the Electromagnetic CALorimeter at the ILC" *JINST* **6** (2011) C12040.

[22] L. Royer, J. Bonnard, S. Manen, P. Gay, and X. Soumpholphakdy, "CALORIC : A readout chip for high granularity calorimeter" *IEEE Conf.Publ.* (2011) .

[23] F. Rarbi, D. Dzahini, and L. Gallin-Martel, "A power efficient 12-bit and 25-MS/s pipelined ADC for the ILC/Ecal integrated readout" *IEEE Trans.Nucl.Sci.* **57** (2010) 2798–2804.

[24] L. Gallin-Martel *et al.*, "Design of High Dynamic Range Digital to Analog Converters for the Calibration of the CALICE Si-W Ecal readout electronics" *Topical Workshop on Electronics for Particle Physics* (2009) .

[25] R. Cornat, "Acquisition system and detector interface for power pulsed Acquisition System and Detector Interface for Power Pulsed Detectors" *Physics Procedia* **37** (2012) no. 0, 1791.

[26] J. Rouene, "Construction and testing of a large scale prototype of a silicon tungsten electromagnetic calorimeter for a future lepton collider" *Nucl.Instrum.Meth.* **A732** (2013) 470–474.

[27] T. H. Tran, V. Balagura, V. Boudry, and J.-C. Brient, "Optimization of ild ecal dimensions" in *International Workshop on Future Linear Colliders (LCWS13), 11-15 Nov 2013. Tokyo, Japan* [50]. `https://agenda.linearcollider.org/getFile.py/access?contribId=67&sessionId=35&resId=0&materialId=slides&confId=6000`.

[28] Chihiro Kozakai, Shion Chen, Daniel Jeans and Sachio Komamiya, "Robustness of a siecal used in particle flow reconstruction" in *International Workshop on Future Linear Colliders (LCWS13), 11-15 Nov 2013. Tokyo, Japan* [50].

[29] D. Jeans, J. Brient, and M. Reinhard, "GARLIC : GAmma Reconstruction at a LInear Collider experiment" *JINST* **7** (2012) P06003, `arXiv:1203.0774 [physics.ins-det]`.

[30] I. Laktineh, "Tracking in hadronic showers in the sdhcal prototype using hough transform" in *International Workshop on Future Linear Colliders (LCWS13), 11-15 Nov 2013. Tokyo, Japan* [50].

[31] M. Ruan, "Particle flow algorithm with a digital hcal" in *Proceedings CHEF'2013*. 2013.

[32] M. Ruan, V. Boudry, J. Brient, D. Jeans, and H. Videau, "Fractal dimension analysis in a highly granular calorimeter" in *14th International Workshop on Advanced Computing and Analysis Techniques in Physics Research (ACAT 2011), 5-9 Sep 2011. Uxbridge, West London, UK*, vol. 368, p. 012038. 2011.

[33] M. Bedjidian, K. Belkadhi, V. Boudry, C. Combaret, D. Decotigny, *et al.*, "Performance of Glass Resistive Plate Chambers for a high granularity semi-digital calorimeter" *JINST* **6** (2011) P02001, `arXiv:1011.5969 [physics.ins-det]`.

[34] M. Bedjidian, J. Ianigro, R. Kieffer, I. Laktineh, N. Lumb, *et al.*, "Glass resistive plate chambers for a semi-digital HCAL" *Nucl.Instrum.Meth.* **A623** (2010) 120–122.

[35] L. Caponetto, C. Combaret, C. de la Taille, F. Dulucq, R. Kieffer, *et al.*, "First test of a power-pulsed electronics system on a GRPC detector in a 3-Tesla magnetic field" *JINST* **7** (2012) P04009, `arXiv:1111.5630 [physics.ins-det]`.

[36] C. Adloff, D. Attie, J. Blaha, S. Cap, M. Chefdeville, *et al.*, "MICROMEGAS chambers for hadronic calorimetry at a future linear collider" *JINST* **4** (2009) P11023, `arXiv:0909.3197 [physics.ins-det]`.

[37] C. Adloff, J. Blaha, M. Chefdeville, A. Dalmaz, C. Drancourt, *et al.*, "Construction and test of a 1×1 m^2 Micromegas chamber for sampling hadron calorimetry at future lepton colliders" *Nucl.Instrum.Meth.* **A729** (2013) 90–101.

[38] O. Ferreira, "ILD Seismic design for ILD Detectors". ILD WebEx Integration Meeting – March 2 nd 2012.

[39] P. Mora de Freitas and H. Videau, "Detector simulation with MOKKA / GEANT4 : Present and future". LC-TOOL-2003-010.

[40] P. Mato, "Software design for geomtry toolkit" Tech. Rep. AIDA-D2.3, August, 2012. `http://cds.cern.ch/record/1473120/files/AIDA-D2_3.pdf?version=1`.

[41] G. Alexander, F. Badaud, M. Battaglia, T. Behnke, M. Berggren, *et al.*, "TESLA : The superconducting electron positron linear collider with an integrated X-ray laser laboratory. Technical design report. Pt. 4 : A detector for TESLA". `http://flash.desy.de/tesla/tesla_documentation#e1509`.

[42] C. Bourgeois and A. Gonnin, "Integration of inner detector region". `http://edmsdirect.desy.de/edmsdirect/file.jsp?edmsid=D00000001003815,A,1,1`. EDMS-ID : D*1003815,A,1,1.

[43] in *ILD MDI/Integration Pre-Meeting*. 2012. `http://agenda.linearcollider.org/conferenceDisplay.py?confId=5611`.

[44] Catherine Clerc, "Status of Cable Paths and Patch Panels studies" in *ILD MDI/Integration Pre-Meeting* [43]. `http://agenda.linearcollider.org/conferenceDisplay.py?confId=5611`.

[45] J. Ianigro, "Sdhcal barrel and endcap issues" in *ILD MDI/Integration Pre-Meeting* [43]. `http://agenda.linearcollider.org/conferenceDisplay.py?confId=5611`.

[46] H. Perrey, "An eudet/aida pixel beam telescope for detector development" *IEEE NSS/MIC, Anaheim (CA, USA) Oct - Nov 2012* (2012) .

[47] C. Schrader, S. Amar-Youcef, N. Bialas, M. Deveaux, I. Frohlich, *et al.*, "A demonstrator for the micro-vertex-detector of the CBM experiment" *PoS* **BORMIO2010** (2010) 017.

[48] M. Boezio, V. Bonvicini, E. Mocchiutti, P. Schiavon, G. Scian, *et al.*, "A High granularity imaging calorimeter for cosmic ray physics" *Nucl.Instrum.Meth.* **A487** (2002) 407–422, `arXiv:physics/0109010 [physics]`.

[49] E. Obrien, S. Boose, M. Chiu, B. Johnson, E. Kistenev, D. Lynch, R. Nouicer, R. Pak, R. Pisani, S. Stoll, *et al.*, "Technical Design Report for a Nosecone Calorimeter (NCC) for the PHENIX Experiment." tech. rep., Brookhaven National Laboratory, 2007. `http://www.bnl.gov/isd/documents/36694.pdf`.

[50] in *International Workshop on Future Linear Colliders (LCWS13), 11-15 Nov 2013. Tokyo, Japan.* November, 2013.

A PhD theses on ILC detector and physics studies since 2008

Liste provisoirement restreinte à l'IPHC à l'IPNL, au LAL, au LLR et au LPSC.

1. Theses on physics studies
   - H. Li, *Higgs Recoil Mass and Cross-Section Analysis at ILC and Calibration of the CALICE SiW ECAL Prototype*, LAL, 2006-2009
   - P. Doublet, *Hadrons dans un calorimètre électromagnétique silicium-tungstène hautement granulaire Production du quark top à l'International Linear Collider*, LAL, 2008-2011
   - M. Ruan, *A precise Higgs mass measurement at the ILC and test beam data analyses with CALICE*, LAL and Tsinghua, 2005-2008
   - M. Reinhard, *P violation in the Higgs sector with a next-generation detector at the ILC*, LLR, 2007-2009
   - J. Rouëné, *Top quark and Ecal tech. prototype*, LAL, 2011-2014
   - M.S. Amjad, *Forward backward asymmetry in top quark production at the ILC*, LAL, 2012-2014
2. Theses on vertex detectors
   - S. Heini, *Development of a highly granular, swift and radiation tolerant monolithic pixel sensor*, IPHC, 2004 - 2009
   - M. Dahoumane, *Conception, réalisation et caractérisation de l'électronique intégrée de lecture et de codage des signaux des détecteurs de particules chargées à pixels actifs en technologie CMOS*, IPHC et LPSC, 2005 - 2009
   - N. Pillet, *Optimisation de la chaîne de lecture des capteurs CMOS*, IPHC, 2006 - 2009
   - O. Torheim, *Design and implementation of fast and sparsified readout for Monolithic Active Pixel Sensors*, IPHC and Bergen University, 2007 - 2010
   - Y. Fu, *Développement de capteurs à pixel CMOS pour un détecteur de vertex adapté au collisionneur ILC*, IPHC, 2009 - 2012
   - G. Voutsinas, *Optimization of a vertex detector for the ILC and study of the Higgs boson couplings*, IPHC, 2008-2012
   - L. Cousin, *Trajectométrie dans le cadre du projet européen AIDA et optimisation du détecteur de vertex équipé de capteurs CMOS de l'expérience SuperB*, IPHC, 2011 - 2014
   - J. Wang, *Design and development of low-power and low-noise power management circuitry in CMOS pixel sensors*, IPHC, 2009-2012
   - L. Zhang, *Recherche de nouvelles architectures électroniques pour capteurs monolithiques du type pixel actif en 3D (3DLTMAPS)*, IPHC, 2008-2013
   - T. Wang, *Towards computational 3D integrated. low noise very large scale CMOS pixel sensors for High Energy Physics applications*, IPHC, 2011-
   - W. Zao, *Design and development of a low noise, low power, radiation tolerance power supply chip for particle detection systems*, IPHC, 2010-
3. Theses on the silicon tungsten Ecal
   - L. Morin, *Etude du calorimètre électromagnétique silicium-tungstène du concept de détecteur ILD pour l'ILC et mesure de la masse du boson de Higgs dans le canal $e^+e^- \to ZH \to e^+e^- + X$*, LPSC, 2006-2010
   - F.-E. Rarbi, *Conception d'un convertisseur analogique numérique pipeline de grande dynamique et de faible consommation pour le codage des signaux de détecteurs à forte granularité*, LPSC, 2007-2010
4. Theses on the Semi-Digital Hcal
   - K. Belkadhi *Étude d'une calorimétrie hadronique semi-digitale pour l'ILC*, LLR, 2008-2012 (non soutenue).

- R. Kieffer, *Caractérisation d'un calorimìtre hadronique semi-digital pour le futur collisionneur*, IPNL, 2008-2011
- Y. Haddad, *Performance d'une calorimètre hadronique ultra-granulaire pour l'étude du Higgs en* $e^+e^- \to HZ$; $Z \to q\bar{q}$, LLR, 2011-
- A. Steen, *Etudes des gerbes hadroniques à l'aide du prototype calorimètre hadronique à lecture semi-digitale (SDHCAL). Etude du canal* $\mathrm{e}^+\mathrm{e}^- \to WW$ *dans le détecteur ILD*, IPNL, 2012-
- R. Été, *Développement d'algorithmes PFA dans le cadre du détecteur ILD avec un calorimet̀re hadronique à lecture semi-digitale (SDHCAL). Etude du boson Higgs à l'aide du canal* $\mathrm{e}^+\mathrm{e}^- \to HZ$, IPNL, 2012-

B Staff and budget since 2008

FIGURE 23 – Staff evolution since 2008.

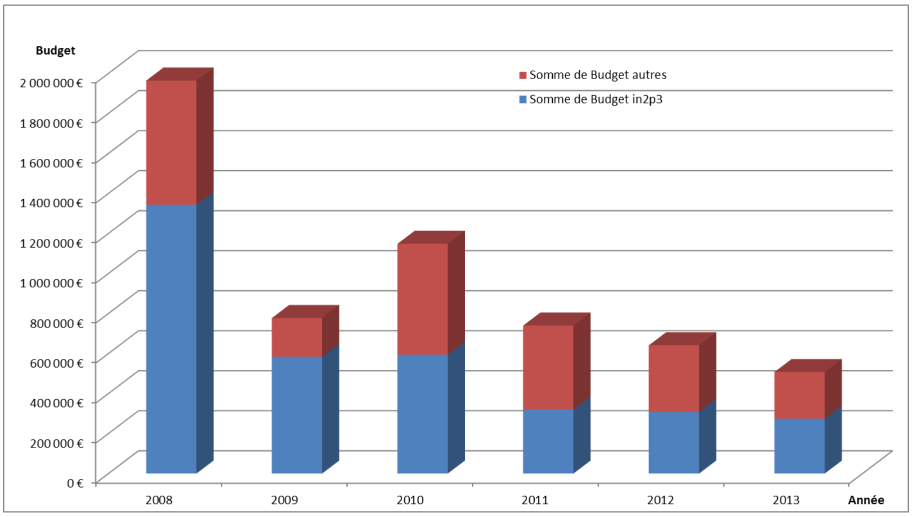

FIGURE 24 – Budget evolution since 2008.

Labo	Année	Ressources Colisionneurs Linéaires (FTE et Euros) Nombre de Physiciens	Nombre de ITA	Nombre de Post Docs	Nombre d' Etudiants	Somme de Budget in2p3	Somme de Budget autres
IPHC	2008	1,2	15,0	0,5	4,0	155 000 €	361 000 €
	2009	1,2	15,0	1,0	4,0	132 000 €	0 €
	2010	1,7	15,0	1,0	4,0	121 000 €	197 000 €
	2011	1,2	7,0	0,0	3,0	47 000 €	182 000 €
	2012	0,8	5,0	0,0	3,0	40 000 €	141 000 €
	2013	0,8	4,0	0,0	2,0	43 000 €	64 000 €
Total IPHC		**6,9**	**61,0**	**2,5**	**20,0**	**538 000 €**	**945 000 €**
IPNL	2008	2,7	6,0	1,0	1,0	110 000 €	1 000 €
	2009	3,0	5,7	0,4	1,5	70 700 €	20 100 €
	2010	3,6	8,0	1,4	2,0	134 000 €	128 000 €
	2011	3,5	8,1	1,0	1,5	63 000 €	4 750 €
	2012	2,2	4,6	1,1	1,1	63 500 €	10 200 €
	2013	2,2	4,6	1,0	1,7	55 000 €	27 600 €
Total IPNL		**17,2**	**36,9**	**5,9**	**8,7**	**496 200 €**	**191 650 €**
LAL	2008	2,1	5,5	1,0	1,5	384 000 €	86 768 €
	2009	0,0	4,4	2,0	1,8	98 000 €	0 €
	2010	0,0	4,7	2,0	1,0	112 000 €	0 €
	2011	0,3	4,8	1,8	1,0	49 300 €	16 118 €
	2012	1,0	4,8	1,3	2,0	44 200 €	39 676 €
	2013	1,4	1,4	1,5	2,0	43 800 €	28 000 €
Total LAL		**4,8**	**25,4**	**9,5**	**9,3**	**731 300 €**	**170 562 €**
LAPP	2008	0,7	5,2	0,7	0,3	150 000 €	27 622 €
	2009	1,2	6,6	2,0	1,0	58 300 €	52 622 €
	2010	1,2	6,2	2,0	1,0	56 450 €	17 622 €
	2011	1,6	5,7	1,5	0,8	52 716 €	105 903 €
	2012	3,4	4,1	1,0	0,0	49 000 €	77 947 €
	2013	2,4	2,3	0,9	0,0	31 000 €	52 947 €
Total LAPP		**10,5**	**30,1**	**8,1**	**3,0**	**397 466 €**	**334 664 €**
LLR	2008	4,0	7,3	0,5	1,2	250 000 €	31 324 €
	2009	5,6	7,3	1,9	2,0	91 300 €	40 700 €
	2010	5,7	7,6	3,0	2,0	80 200 €	119 000 €
	2011	5,8	7,8	2,7	1,6	51 000 €	106 833 €
	2012	4,7	7,6	3,0	1,4	54 000 €	59 833 €
	2013	5,3	5,8	2,0	1,0	62 500 €	55 633 €
Total LLR		**31,1**	**43,4**	**13,1**	**9,2**	**589 000 €**	**413 324 €**
LPC	2008	1,7	3,3	2,0	1,0	12 500 €	8 000 €
	2009	1,5	3,0	2,0	1,0	12 500 €	4 000 €
	2010	1,1	2,0	1,0	0,5	20 000 €	4 000 €
	2011	0,5	2,3	0,0	0,5	15 000 €	3 000 €
	2012	0,3	1,0	0,0	0,0	3 000 €	0 €
	2013	0,3	0,4	0,0	0,0	3 000 €	0 €
Total LPC		**5,3**	**12,0**	**5,0**	**3,0**	**66 000 €**	**19 000 €**
LPNHE	2008	1,2	4,4	1,0	1,0	155 000 €	104 767 €
	2009	2,2	5,8	2,0	1,0	44 400 €	76 566 €
	2010	2,9	4,6	1,0	0,0	35 000 €	88 979 €
	2011	1,0	1,0	0,0	0,0	13 000 €	0 €
	2012	1,0	1,2	0,0	0,0	37 500 €	0 €
	2013	0,9	1,6	0,0	0,0	20 000 €	0 €
Total LPNHE		**9,2**	**18,5**	**4,0**	**2,0**	**304 900 €**	**270 312 €**
LPSC	2008	0,7	1,9	0,0	2,0	127 000 €	0 €
	2009	0,9	3,0	1,0	2,0	76 000 €	0 €
	2010	0,8	2,7	1,0	1,1	35 000 €	0 €
	2011	0,8	1,4	0,0	0,0	30 000 €	0 €
	2012	0,7	1,3	0,0	0,0	17 000 €	4 000 €
	2013	0,6	0,8	0,0	0,0	16 000 €	5 000 €
Total LPSC		**4,5**	**11,0**	**2,0**	**5,1**	**301 000 €**	**9 000 €**
Total général		**89,4**	**238,3**	**50,1**	**60,4**	**3 423 866 €**	**2 353 512 €**

FIGURE 25 – Details on budget and staff working at the IN2P3 institutes on ILC detector development and physics studies since 2008.